Available online at www.sciencedirect.com

ScienceDirect

Geochimica et Cosmochimica Acta 75 (2011) 427–443

Geochimica et Cosmochimica Acta

www.elsevier.com/locate/gca

Controls on calcium isotope fractionation in cultured planktic foraminifera, *Globigerinoides ruber* and *Globigerinella siphonifera*

B. Kısakürek [a,*], A. Eisenhauer [a], F. Böhm [a], E.C. Hathorne [a,b], J. Erez [c]

[a] *Leibniz-Institut für Meereswissenschaften, IFM-GEOMAR, Wischhofstr. 1-3, D 24148 Kiel, Germany*
[b] *MARUM – Center for Marine Environmental Sciences, University of Bremen, Leobener Str., D 28359 Bremen, Germany*
[c] *Department of Earth Sciences, The Hebrew University of Jerusalem, 91904 Jerusalem, Israel*

Received 12 August 2009; accepted in revised form 18 October 2010; available online 27 October 2010

Abstract

Specimens of two species of planktic foraminifera, *Globigerinoides ruber* and *Globigerinella siphonifera*, were grown under controlled laboratory conditions at a range of temperatures (18–31 °C), salinities (32–44 psu) and pH levels (7.9–8.4). The shells were examined for their calcium isotope compositions ($\delta^{44/40}$Ca) and strontium to calcium ratios (Sr/Ca) using Thermal Ionization Mass Spectrometry and Inductively Coupled Plasma Mass Spectrometry. Although the total variation in $\delta^{44/40}$Ca (~0.3‰) in the studied species is on the same order as the external reproducibility, the data set reveals some apparent trends that are controlled by more than one environmental parameter. There is a well-defined inverse linear relationship between $\delta^{44/40}$Ca and Sr/Ca in all experiments, suggesting similar controls on these proxies in foraminiferal calcite independent of species. Analogous to recent results from inorganically precipitated calcite, we suggest that Ca isotope fractionation and Sr partitioning in planktic foraminifera are mainly controlled by precipitation kinetics. This postulation provides us with a unique tool to calculate precipitation rates and draws support from the observation that Sr/Ca ratios are positively correlated with average growth rates. At 25 °C water temperature, precipitation rates in *G. siphonifera* and *G. ruber* are calculated to be on the order of 2000 and 3000 μmol/m^2/h, respectively. The lower $\delta^{44/40}$Ca observed at $\geqslant$29 °C in both species is consistent with increased precipitation rates at high water temperatures. Salinity response of $\delta^{44/40}$Ca (and Sr/Ca) in *G. siphonifera* implies that this species has the highest precipitation rates at the salinity of its natural habitat, whereas increasing salinities appear to trigger higher precipitation rates in *G. ruber*. Isotope effects that cannot be explained by precipitation rate in planktic foraminifera can be explained by a biological control, related to a vacuolar pathway for supply of ions during biomineralization and a pH regulation mechanism in these vacuoles. In case of an additional pathway via cross-membrane transport, supplying light Ca for calcification, the $\delta^{44/40}$Ca of the reservoir is constrained as −0.2‰ relative to seawater. Using a Rayleigh distillation model, we calculate that calcification occurs in a semi-open system, where less than half of the Ca supplied by vacuolization is utilized for calcite precipitation. Our findings are relevant for interpreting paleo-proxy data on $\delta^{44/40}$Ca and Sr/Ca in foraminifera as well as understanding their biomineralization processes.

1. INTRODUCTION

Early investigations by Zhu and MacDougall (1998) suggested that variations in calcium (Ca) isotope composition of certain foraminifera may be controlled by temperature. This was confirmed by $\delta^{44/40}$Ca-temperature calibrations of cultured and field-collected specimens of one species of planktic foraminifera, *Globigerinoides sacculifer*, which demonstrated a temperature sensitivity on the order of 0.2‰/°C (Nägler et al., 2000; Hippler et al., 2006). This temperature relationship was applied to down-core records coupled with other proxies (Mg/Ca and δ^{18}O) to extract past sea surface

* Corresponding author. Tel.: +49 431 6002111; fax: +49 431 6002928.
E-mail address: bkisakurek@ifm-geomar.de (B. Kısakürek).

0016-7037/$ - see front matter © 2010 Elsevier Ltd. All rights reserved.
doi:10.1016/j.gca.2010.10.015

temperatures (Nägler et al., 2000; Hippler et al., 2006) and salinities (Gussone et al., 2004).

Other studies on core-tops and laboratory cultures demonstrated that Ca isotope fractionation in planktic foraminifera is species-dependent, wherein the temperature sensitivity for most planktic species is an order of magnitude lower than that for *G. sacculifer* (Gussone et al., 2003, 2009; Griffith et al., 2008). This temperature sensitivity on the order of 0.02‰/°C was confirmed for other calcifying organisms such as corals (Böhm et al., 2006) and coccolithophores (Gussone et al., 2006, 2007) as well as for inorganic aragonite and calcite (Gussone et al., 2003; Marriott et al., 2004). Ca isotope records of those species of foraminifera with less temperature sensitivity were used to investigate secular $\delta^{44/40}$Ca variations in seawater (De La Rocha and DePaolo, 2000; Heuser et al., 2005; Sime et al., 2007).

A study by Sime et al. (2005) and a recent compilation by Kasemann et al. (2008) found no significant correlation between temperature and the Ca isotope composition of more than twelve species of planktic foraminifera (including *G. sacculifer*) from core-top sediments. A record of Ca isotope composition of *G. sacculifer* from ODP site 925 in the Atlantic has been shown to closely follow that of several other species of planktic foraminifera and lacks the large variability expected if temperature was a significant driver (Sime et al., 2007). Ca isotope data on *G. sacculifer* from core-tops (Chang et al., 2004; Griffith et al., 2008) and culture experiments (Gussone et al., 2009) failed to reproduce the large temperature-dependent fractionation established by samples from plankton tows and previous culturing experiments (Nägler et al., 2000; Hippler et al., 2006). Gussone et al. (2009) examined the causes of the contrasting Ca isotope fractionation behaviour in *G. sacculifer* from culturing experiments conducted by Hemleben et al. (1987, 1989) in different seasons in Barbados. Specimens with a weak temperature dependence of Ca-isotope ratios (Gussone et al., 2009) were grown under low salinity conditions (33–34.5) and displayed growth limitations such as smaller test diameter, shorter survival time and reduced prey acceptance prior to gametogenesis. In contrast, specimens with a strong temperature response (Nägler et al., 2000) were cultured at high salinities (34.5–36), where they grew to bigger sizes, accepted more food and had a higher frequency of gametogenesis. The bimodal temperature sensitivity within a single species was also observed in *Neogloboquadrina pachyderma* (sin.) from plankton tows and core-top sediments (Gussone et al., 2009; Hippler et al., 2009; Kozdon et al., 2009). The strong temperature sensitivity of Ca isotope fractionation in *N. pachyderma* (on the order of 0.2‰/°C) was observed to have an offset between different water masses (Gussone et al., 2009) or to break down below a critical threshold temperature of ~2–3 °C and salinity of ~33–34 (Hippler et al., 2009; Kozdon et al., 2009). This shift in behaviour was observed to be independent of genetic variations (Hippler et al., 2009). Kozdon et al. (2009) observed that Ca-isotope ratios and Mg/Ca ratios in *N. pachyderma* (sin.) reflect water temperatures (>2.5 °C) along isopycnal layers in the Norwegian Sea, whereas an impaired temperature response of both proxies in the polar regions was hypothesized to be associated with high calcification rates in *N. pachyderma* (sin.) in cold waters (<2.5 °C). Griffith et al. (2008) observed that sediment trap samples of *Globigerinoides ruber* and *Globigerinoides sacculifer* show a large degree of Ca isotope fractionation at high temperatures (>27 °C), deviating from the temperature-dependent fractionation trend followed by core-top samples. Thus it is now apparent that there are additional controls other than temperature on Ca isotope fractionation in planktic foraminifera and that growth effects might be important.

High spatial resolution *in situ* Ca isotope measurements on planktic foraminifera using ion microprobe revealed intra-test $\delta^{44/40}$Ca variations of 1.7‰ in *Globorotalia inflata* (Rollion-Bard et al., 2007), 1.6‰ in *Globorotalia truncatulinoides* and 3.7‰ in *Globorotalia tumida* (Kasemann et al., 2008), as compared to the total glacial–interglacial variation in planktic foraminiferal $\delta^{44/40}$Ca of ~1.8‰ (Kasemann et al., 2008 and references therein). The intra-test variability in *G. truncatulinoides* and *G. tumida* was observed to be associated with ontogenic versus gametogenetic layers. The gametogenetic layer was found to be isotopically lighter than the ontogenic calcite in *G. tumida*, supporting a temperature influence during precipitation of gametogenetic calcite in deeper and colder waters. In contrast, the gametogenetic layer was shown to be isotopically heavier than the ontogenic calcite in *G. truncatulinoides*. This was hypothesized to result from a kinetic effect or Rayleigh-type fractionation from an internal reservoir (Kasemann et al., 2008).

To better constrain these controls we analyzed Ca isotopes and strontium to calcium ratios (Sr/Ca) in the shells of planktic foraminifera *G. ruber* (white) and *G. siphonifera* collected from the Gulf of Eilat (Red Sea) and cultured under different salinity, temperature and carbonate chemistry conditions. We find a significant correlation between $\delta^{44/40}$Ca and Sr/Ca in the samples from all experiments, suggesting that these ratios are controlled by similar processes. Results from a series of recent inorganic precipitation experiments (Tang et al., 2008a,b,c) display a similar relationship suggesting precipitation kinetics mainly control Ca isotope fractionation in foraminifera.

2. METHODS

2.1. Experimental setup

Foramifera culturing experiments were carried out under controlled laboratory conditions at the Interuniversity Institute for Marine Sciences in Eilat (IUI), Israel. The culturing setup and sample treatment are explained in detail in a related article (Kısakürek et al., 2008). *G. ruber* (white) and *G. siphonifera* were collected from the surface waters (top 20 meters) of the northern Gulf of Eilat via plankton net (102 μm mesh size) between April and July 2006 and between April and May 2007. A wide range of physiological, morphological and genetic lines of evidence indicate that there are two main phenotypes of *G. siphonifera* (Type I and II) and that these two types can be considered as distinct cryptic species (Faber et al., 1988, 1989; Darling

et al., 1997; Huber et al., 1997; de Vargas et al., 2002; Darling and Wade, 2008). According to the genetic sequencing study of de Vargas et al. (2002), *G. siphonifera* specimens collected from the surface waters (between 175 m depth and the sea surface) of the northern Gulf of Eilat in May 1999 belong to Genotype II (i.e., Type IIa according to the revised system of Darling and Wade, 2008). Our study does not involve genetic investigations on *G. siphonifera* from the Gulf of Eilat, mainly because of the difficulties associated with performing coupled analysis on shell chemistry and DNA sequencing.

Foraminifera were picked from the tow sample using a binocular microscope. A small fraction was kept as a control group, whereas the recovered specimens were cultured individually in 100 ml Erlenmeyer flasks filled with Gulf of Eilat seawater filtered to 0.45 μm and fed one newly hatched brine shrimp (*Artemia* sp.) every day. The flasks were kept tightly capped and placed in temperature controlled water baths with ±0.2 °C precision. Light was provided artificially for 14 h a day (followed by dark phase of 10 h) by a metal halide type lamp (420 W, Osram™) at a constant irradiance of 200 μmol photons m^{-2} s^{-1}. Upon gametogenesis the shell was rinsed five times in distilled water and dried before its diameter and weight were measured. The culturing fluids were sampled using a plastic syringe, filtered to 0.2 μm and stored below 10 °C in the dark for chemical analysis.

Each experimental setup simulated variations in a single environmental parameter (i.e., temperature, salinity or carbonate chemistry of seawater) while keeping others constant. The range of these environmental parameters was designed to cover the variability in the natural habitat of *G. ruber* and *G. siphonifera*. Two to six foraminifera of a single species were cultured in each experimental setup (Table 1).

Temperature and salinity experiments (BK1, BK2 and BK4 experiments in Table 1) were conducted on both species and covered a range from 18 to 31 °C and from 32 to 44 psu, respectively. Salinity was altered either by adding distilled water to seawater for lower salinities or by evaporating for higher salinities. Carbonate system parameters of these experiments were estimated using the computer program written by Lewis and Wallace (1998) by assuming that total alkalinity and total inorganic carbon (2490 μeq/l and 2060 μmol/kg, respectively, at a salinity of 40.7 psu in the northern part of the Gulf of Eilat; Silverman et al., 2007) behave conservatively with changing salinity (Table 1).

In an additional set of experiments on *G. ruber* (BK3 experiments in Table 1), the carbonate system was manipulated so that total inorganic carbon (C_T) was kept constant by allowing no exchange with the atmosphere while pH and carbonate ion concentration ($[CO_3^{2-}]$) were altered through the addition of dilute (0.05 M, reagent grade) HCl or NaOH. Before the adjustment of pH, the Gulf of Eilat seawater was bubbled with ambient air overnight to equilibrate with atmospheric CO_2 and its salinity was adjusted to 35 psu by addition of distilled water, which contains no alkalinity and a negligible amount of inorganic carbon. The culturing fluids from the carbonate chemistry experiments were analyzed for total alkalinity and total inorganic carbon (Kısakürek et al., 2008), allowing the other carbonate system parameters (e.g., $[CO_3^{2-}]$, pH) to be accurately calculated using the computer program written by Lewis and Wallace (1998), using K1 and K2 constants from Mehrbach et al. (1973) refitted by Dickson and Millero (1987) and K_{SO4} constant from Dickson (1990). Accordingly, the carbonate chemistry experiments encompassed a $[CO_3^{2-}]$ range of 140–380 μmol/l and a pH range of 7.9–8.4 (Table 1).

One specimen of *G. ruber* (cultured at 30 °C) and two specimens of *G. siphonifera* (one cultured at the Gulf of Eilat salinity of 40.7 psu and the other one at 32.1 psu) were embedded in epoxy resin, polished to expose a cross-section through the test, coated with carbon and examined for semi-quantitative distribution patterns of Sr/Ca (elemental map) on a JEOL JXA 8200 electron microprobe at the Leibniz Institute of Marine Sciences (IFM-GEOMAR).

Shells from repeat experiments were grouped together and transferred into a pre-cleaned micro centrifuge tube for sample cleaning. Given that organics might cause isobaric interferences during Ca isotope analysis (Heuser et al., 2005), the foraminifera tests were cleaned of residual organic matter by oxidation in dilute sodium hypochlorite solution (reagent grade, Sigma Aldrich, diluted 1:20 or <1% active reagent). The vials were repeatedly shaken by a vortex shaker. After employing several washes with ultrapure water, the samples were dissolved in 10 μL of ultrapure 2.5 N HCl, transferred at once to Savillex beakers, evaporated and redissolved in ultrapure 2.5 N HCl with a concentration of ~160 μg of Ca per ml of sample solution.

Our approach was to group all cultured specimens in an experiment together in order to minimize intra-specific variability. In this manner, growth rates were calculated as an average for each experiment (Table 1). To do this, we calculated first the growth rate (GR) of each cultured specimen (Eqs. (1) and (2)) and then the average growth rate (μg/day/ind and %/day/ind) by taking the arithmetic mean of all GR in an experimental setup. The errors on average growth rates are given in two standard errors of the mean ($2\sigma_m$) calculated for the number of cultured specimens grouped together in an experiment (Table 1).

$$\mathrm{GR}\ (\mu g/\mathrm{day}) = [m_f\ (\mu g) - m_i\ (\mu g)]/\Delta t\ (\mathrm{day}), \quad (1)$$

where the growth of a foraminifera is assumed to be linear across the duration of an experiment, m_f and m_i stand for final and initial shell masses, consecutively.

$$\mathrm{GR}\ (\%/\mathrm{day}) = \ln[m_f\ (\mu g)/m_i\ (\mu g)]/\Delta t\ (\mathrm{day}) * 100, \quad (2)$$

where the growth is assumed to be exponential across the duration of an experiment.

Final shell mass was measured using a Kahn microbalance, whereas initial shell mass was estimated from the size versus mass relationship given in Fig. 1. The duration of the experiment (Δt) denotes the number of days from when the foraminifera was first fed until gametogenesis. The first feeding was carried out 1–4 days after the collection date, depending on the recovery of specimens.

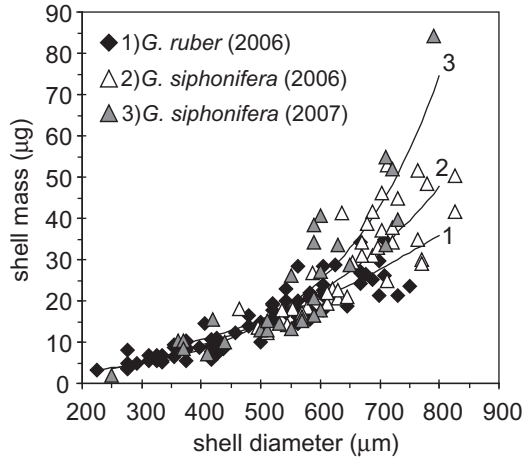

Fig. 1. Species specific correlation between shell diameter (D) and mass (m) for (1) *G. ruber* [$m = 0.00008 * D^{1.95}$, $R^2 = 0.89$)], (2) 2006 cultures of *G. siphonifera* [$m = 2.34 * \exp(0.0038 * D)$, $R^2 = 0.71$)], and (3) 2007 cultures of *G. siphonifera* [$m = 0.93 * \exp(0.0055 * D)$, $R^2 = 0.83$)]. The final mass of the shell of each cultured specimen was determined using a Kahn microbalance with a precision of ±0.1 µg, whereas the final diameter (>300 µm) was assessed under an inverted microscope. The lower end of the correlations rely on control specimens (having diameter <300 µm). These correlations allow for the estimation of the mass of each specimen at the start of the experiment (i.e., initial mass) given that its initial diameter was determined on a binocular microscope. A power-type regression was preferred over an exponential one in *G. ruber* because the fit better approximates for low shell mass. The higher exponent of *G. siphonifera* cultured in 2007 compared to 2006 appears to be due to the better adaptation of this species to the natural salinity of the Gulf of Eilat (~41 psu; see Table 1 and Section 3.2).

2.2. Calcium isotope measurements

Ca isotopes were measured on a Finnigan TRITON Thermal Ionization Mass Spectrometer (TIMS) at the IFM-GEOMAR, following the method described in Heuser et al. (2002). Briefly, an aliquot of the sample HCl dissolution comprising ~300 ng Ca was spiked with a known amount of $^{43}Ca/^{48}Ca$ double spike solution, evaporated to dryness and then loaded with 2 N HCl and $TaCl_5$ activator onto a zone-refined Re single filament. Samples were heated to a temperature of approximately 1500 °C, corresponding to a signal intensity of 4–5 V on ^{40}Ca. Measurements were made in dynamic mode with $^{40}Ca/^{43}Ca$, $^{42}Ca/^{43}Ca$, and $^{44}Ca/^{43}Ca$ measured in the main cycle and $^{43}Ca/^{48}Ca$ in the second cycle. The procedural blank of this technique yields less than 4.5 ng Ca (<1.5% of the sample size).

The Ca isotope data are expressed relative to NIST SRM915a standard as $\delta^{44/40}Ca = [(^{44}Ca/^{40}Ca)_{sample}/(^{44}Ca/^{40}Ca)_{SRM915a} - 1] \times 1000$ (Eisenhauer et al., 2004). The $\delta^{44/40}Ca$ values for each analytical session were calculated relative to the mean of the SRM915 standards run in that session. The average precision of SRM915a standards ($n = 4$) run during a session was 0.1–0.2‰ ($2\sigma_m$). An in-house CaF_2 standard was run in every session. The long term reproducibility of this CaF_2 standard run over 27 sessions over 13 months is $+1.47 \pm 0.24$‰ (2σ, $n = 27$), which is in agreement with previously published values of $+1.45 \pm 0.26$‰ (2σ, $n = 105$; Gussone et al., 2003) and $+1.47 \pm 0.19$‰ (2σ, $n = 30$; Hippler et al., 2003, 2006). The $\delta^{44/40}Ca$ value of each sample reported in this study is the mean of 3–12 repeats (Table 2). These repeats were not analyzed one after another in a single batch, but run in several sessions over the long term (3–4 months). We report the error on each sample in $2\sigma_m$.

Samples of the Gulf of Eilat seawater used for culturing and IAPSO seawater standard were spiked prior to separation of Ca through cation exchange chemistry following the procedure given in Amini et al. (2008). The blank for column chemistry was less than 6 ng Ca (<2% of the sample size). The $\delta^{44/40}Ca$ of seawater from the Gulf of Eilat (i.e., the culturing solutions) was determined as $+1.84 \pm 0.08$‰ ($2\sigma_m$, $n = 13$), which is identical within analytical uncertainty to $\delta^{44/40}Ca$ of IAPSO measured in this study ($+1.78 \pm 0.06$‰, $n = 16$) and in previous studies ($+1.88 \pm 0.04$‰, Hippler et al., 2003; $+1.86 \pm 0.04$‰, Amini et al., 2008). The fractionation of Ca isotopes in calcite relative to the fluid from which it precipitated is expressed as $\Delta^{44/40}Ca = \delta^{44/40}Ca_{calcite} - \delta^{44/40}Ca_{fluid}$. The estimated error on $\Delta^{44/40}Ca$ is on the order of ±0.15‰ ($2\sigma_m$) as propagated from the errors of calcite (±0.1‰ on average; Table 2) and fluid (±0.08‰) composition determinations.

2.3. Sr/Ca analysis

Sr/Ca ratios in *G. ruber* were measured on an Agilent 7500cs series Quadrupole Inductively Coupled Plasma Mass Spectrometry (ICP-MS) at the Institute of Geosciences at the University of Kiel (Kısakürek et al., 2008). Sr/Ca ratios in *G. siphonifera* were measured on a Thermo Scientific Element 2 Sector Field ICP-MS at the University of Bremen. Procedural blanks for Ca and Sr were <0.2% for all samples. Repeat analyses of an in-house standard solution on the Agilent 7500cs and Element 2 gave a precision of ±0.04 mmol/mol (2σ, $n = 8$) and ±0.02 mmol/mol (2σ, $n = 11$), respectively. Cross-calibration of two samples provided an inter-instrumental Sr/Ca precision of ±0.05 mmol/mol (2σ) (Kısakürek et al., 2008). Mixed standard solutions prepared by Greaves et al. (2005) were measured on the Element 2 to check the accuracy. Sr/Ca ratios determined in solutions CL1 and CL7 (2.14 and 1.66 mmol/mol, respectively) are within the inter-instrumental precision (±0.05; 2σ) of the published values (Greaves et al., 2005).

Sr/Ca of the culturing fluids was measured on Jobin Yvon JY 170 Ultratrace series ICP-OES at the IFM-GEOMAR. Sr/Ca of the culturing solutions from the Gulf of Eilat (covering the entire range in salinity and carbonate chemistry experiments) were determined as 8.87 ± 0.11 mmol/mol (2σ; $n = 19$). This is in good agreement with the Sr/Ca ratio of IAPSO measured during the same analytical session (8.79 ± 0.07 mmol/mol; $n = 6$).

3. RESULTS

Shell chemistry data are given in Table 2, where $\delta^{44/40}Ca$ (and Sr/Ca) values of repeat experiments (i.e., BK1-35*R* vs. BK2-24*R*; BK1-35*S* vs. BK2-24*S*, BK1-44*S*_1 vs.

BK1-44*S*_2) are shown to be within error of each other. In a previous study dealing with Mg/Ca ratios in the same samples of *G. ruber*, it was observed that employing a correction on Mg/Ca for the initial mass of foraminifera, calcified in nature, improved the temperature calibration significantly (Kısakürek et al., 2008). However, applying such a correction on $\delta^{44/40}$Ca and Sr/Ca produces values that are identical within analytical uncertainty to the uncorrected values. This is because (i) there is very little variability in both $\delta^{44/40}$Ca and Sr/Ca between the initial mass (as given by the control group of respective species) and the whole test value (Table 2), (ii) the initial mass of the cultured samples constitutes a relatively small portion of the final mass (average proportion of 19% for *G. ruber* and 8% for *G. siphonifera*; Table 1), and (iii) the variability in the dataset is small compared with the external reproducibility of both proxies (Sections 2.2 and 2.3). Thus, in this study we have not employed a correction on $\delta^{44/40}$Ca and Sr/Ca for the initial mass.

3.1. Calcium isotope fractionation

The range of $\delta^{44/40}$Ca in cultured *G. ruber* and *G. siphonifera* (~0.6 to 0.9‰) is in good agreement with previous studies of these species from core-tops and net catches (Sime et al., 2005; Griffith et al., 2008; Kasemann et al., 2008). The total variation in $\delta^{44/40}$Ca is ~0.3‰, which is remarkable considering the large modifications in environmental conditions used in these experiments. Even though this variability is on the same order as the external reproducibility, there are some apparent trends in the data set (Fig. 2a–c).

Our results reveal no linear correlation between temperature and $\delta^{44/40}$Ca in the studied planktic foraminifera (Fig. 2a). The Ca isotope composition is nearly constant at intermediate water temperatures ($\delta^{44/40}$Ca of ~0.7‰ in *G. ruber*; ~0.8‰ in *G. siphonifera*, excluding the outlier at 24 °C), whereas $\delta^{44/40}$Ca decreases (to as low as ~0.6‰) at extremely low and high temperatures. Below 24 °C (Fig. 2a), the positive temperature dependence of $\delta^{44/40}$Ca in *G. ruber* (0.02 ± 0.04‰/°C at 95% confidence level) is essentially consistent with the previously observed temperature sensitivity of ~0.02‰/°C in cultured *Orbulina universa* and inorganic calcite (Gussone et al., 2003; Marriott et al., 2004). At 30–31 °C, the highest temperature at which *G. ruber* and *G. siphonifera* can survive, the lower $\delta^{44/40}$Ca corresponds to a high growth rate in each species (experiments BK2-30*R* and BK4-31*S*; Tables 1 and 2).

Temperature calibration of $\delta^{44/40}$Ca in *G. siphonifera* portrays lower values at the salinity of the Gulf of Eilat (41 psu) than at 35 psu (Fig. 2a). This effect can be tracked in the salinity response of $\delta^{44/40}$Ca in *G. siphonifera*, where culturing at 41 psu produced the lowest $\delta^{44/40}$Ca value (Fig. 2b). We observe no significant response of $\delta^{44/40}$Ca in *G. siphonifera* to changes in salinity including all data points ($R^2 = 0.21$; $p = 0.36$; Fig. 2b). Excluding the data point at 41 psu, the correlation between $\delta^{44/40}$Ca and salinity in *G. siphonifera* improves ($R^2 = 0.85$; $p = 0.03$), but we have no valid reason to exclude this data point.

$\delta^{44/40}$Ca in *G. ruber* decreases with increasing salinity (-0.013 ± 0.009‰/psu; $R^2 = 0.89$; $p < 0.02$; Fig. 2b) and decreasing $[CO_3^{2-}]$ (0.0005 ± 0.0003‰/(μmol/l); $R^2 = 0.97$; $p < 0.02$; Fig. 2c). Since increasing salinities are associated with increasing $[CO_3^{2-}]$ in seawater (Table 1), the observed salinity dependence of $\delta^{44/40}$Ca in *G. ruber* can not be explained by variations of the $[CO_3^{2-}]$. Then again, the change in $\delta^{44/40}$Ca with salinity could be larger than actually observed (if corrected for CO_3^{2-} effect).

The dependence of $\delta^{44/40}$Ca on $[CO_3^{2-}]$ in *G. ruber* has a significant slope of 0.0005 ± 0.0003‰/(μmol/l) (Fig. 2c), whereas a study on cultured *O. universa* found no significant correlation (Gussone et al., 2003). Nevertheless, the range of $\Delta^{44/40}$Ca determined in *G. ruber* (−1.1 to −1.2‰ for $[CO_3^{2-}]$ range of 140–380 μmol/l) agrees well with that in *O. universa* ($\Delta^{44/40}$Ca = −1.0 to −1.2‰; $[CO_3^{2-}]$ = 140–530 μmol/l).

3.2. Sr/Ca ratios

The total variation in Sr/Ca in *G. ruber* and *G. siphonifera* (0.22 mmol/mol; Fig. 2d–f) from all culture experiments is about an order of magnitude higher than the external reproducibly of the measurements (Section 2.3). Sr/Ca increases with increasing temperature (Fig. 2d); calculated slopes (Δ(Sr/Ca)/ΔT) are 0.016 ± 0.003 mmol/mol/°C (95% confidence level; $R^2 = 0.99$; $p < 0.001$) for *G. siphonifera* cultured at 41 psu, 0.008 ± 0.003 mmol/mol/°C ($R^2 = 0.95$; $p = 0.005$) for *G. siphonifera* cultured at 35 psu, and 0.01 ± 0.02 mmol/mol/°C ($R^2 = 0.71$; $p = 0.16$) for *G. ruber* cultured at 35 psu. Previous field calibrations on foraminiferal Sr/Ca did not expose such a clear temperature response in these species (Elderfield et al., 2000; Mortyn et al., 2005). The temperature response of Sr/Ca in *G. siphonifera* is significantly different (calculated for 95% confidence interval) at different salinities (Fig. 2d). At constant temperature, Sr/Ca is higher in *G. siphonifera* cultured at a salinity of 41 psu than at 35 psu (Fig. 2d). This is consistent with the salinity response of Sr/Ca in *G. siphonifera*, where the highest Sr/Ca ratio is observed at 41 psu (Fig. 2e).

Sr/Ca increases with increasing salinity in both *G. ruber* and *G. siphonifera* (Fig. 2e), but the salinity effect on Sr/Ca is not resolvable with high statistical significance ($R^2 = 0.82$ and $p = 0.09$ in *G. ruber*; $R^2 = 0.60$ and $p = 0.07$ in *G. siphonifera*). We observe no significant response of Sr/Ca in *G. ruber* to changes in $[CO_3^{2-}]$ ($R^2 = 0.09$ and $p = 0.70$; Fig. 2f).

3.3. Average growth rate

Culturing studies allow for constraining average growth rates in foraminifera. Variations in average growth rate are shown in Fig. 2g–i along with major trends in shell chemistry (Fig. 2a–f). Our calculations have a large uncertainty (on average ±0.9 μg/day/ind or ±7%/day/ind, $2\sigma_m$) presumably due to individual variability of specimens in one sample as well as errors associated with estimating initial shell mass and duration of the experiment (Section 2.1). Nevertheless, these data are instructive and present some apparent trends as described below.

On the whole, average growth rate varies between 2.0 and 3.5 μg/day/ind (25–35%/day/ind) in the studied species

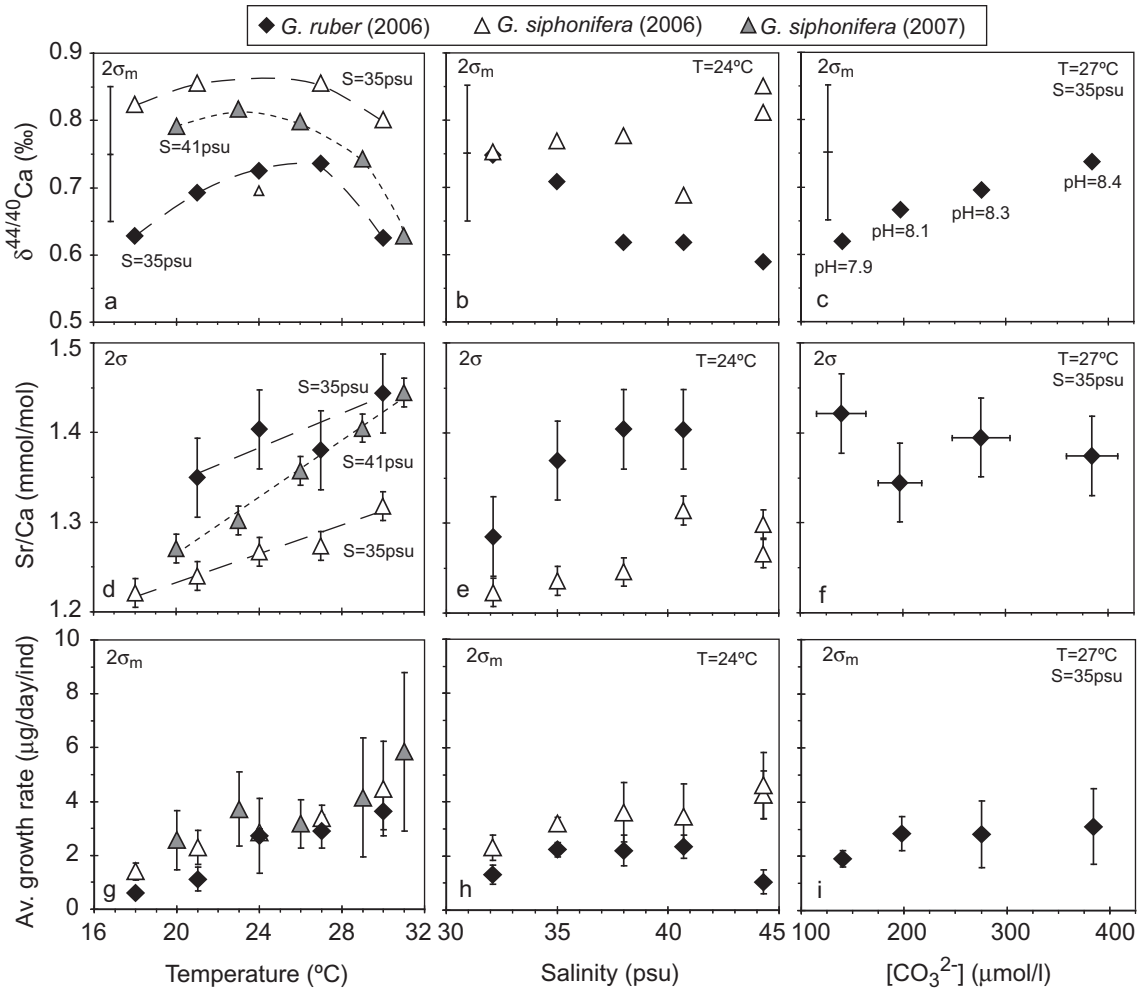

Fig. 2. Variations in shell chemistry ($\delta^{44/40}$Ca and Sr/Ca) and average growth rate of *G. ruber* (diamonds) and *G. siphonifera* (triangles) with temperature, salinity and [CO_3^{2-}]. Temperature experiments were carried out at 35 psu in year 2006, but at the salinity of the Gulf of Eilat (41 psu) in year 2007. All salinity experiments were carried out at 24 °C, whereas carbonate chemistry experiments were carried out at 27 °C and 35 psu. $\delta^{44/40}$Ca of *G. siphonifera* cultured at 24 °C gave an inconsistently low value and has been shown by a small triangle (Fig. 2a). The precision on $\delta^{44/40}$Ca ($2\sigma_m$) is indicated by an average error bar (±0.1‰), whereas individual errors calculated from repeat analysis on each sample are given in Table 2. The error on Sr/Ca is estimated as 2σ from the repeats of an internal standard in two separate sessions for *G. ruber* (±0.04 mmol/mol) and *G. siphonifera* (±0.02 mmol/mol; Section 2.3). The precision on average growth rate ($2\sigma_m$) is calculated for the number of specimens (2–6) grouped together for each sample (Table 1).

at moderate water temperatures (20–27 °C) and moderate salinities (35–41 psu) as well as a wide range of [CO_3^{2-}] (140–380 µmol/l). At a water temperature of 18 °C, average growth rate is considerably low in both *G. ruber* (0.6 µg/day/ind or 17%/day/ind) and *G. siphonifera* (1.4 µg/day/ind or 20%/day/ind). At temperatures ⩾29 °C, average growth rate reaches a plateau with ~3.5 µg/day/ind in *G. ruber* and ~4.5 µg/day/ind in *G. siphonifera* (mainly corresponding to >30%/day/ind for both species). Extreme salinities (32 and 44 psu) induce a lower growth rate in *G. ruber* (~1 µg/day/ind or 20%/day/ind). On the other hand, *G. siphonifera* is well adapted to high salinities (with an average growth rate of ~4.5 µg/day/ind. or ~30%/day/ind at 44 psu), but growth is impaired at low salinities (~2.3 µg/day/ind. or ~20%/day/ind at 32 psu).

Sr/Ca shows a positive correlation with average growth rate (Fig. 3). Results of the carbonate chemistry experiments were excluded from the computation of the regression for *G. ruber* since growth was impaired in this set of experiments, revealing irregular chambers, multiple apertures and unusual patterns of arrangement that do not follow the axis of coiling (Kısakürek et al., 2008).

Plotting Sr/Ca ratios against $\delta^{44/40}$Ca for all samples (Fig. 4) reveals a significant inverse correlation (with a slope of -0.8 ± 0.3‰/(mmol/mol) at 95% confidence level, $R^2 = 0.55$, $p < 0.01$). If each species is examined separately, the correlation between Sr/Ca and $\delta^{44/40}$Ca is still valid ($p \leqslant 0.02$), but obscured due to a smaller number of data points as well as a narrower range of values for a given species (i.e., Sr/Ca = 1.38 ± 0.08 and 1.30 ± 0.13 mmol/mol in *G. ruber* and *G. siphonifera*, respectively; 2σ) compared to all (Sr/Ca = 1.33 ± 0.14; 2σ. Since there is an overlap in data points between the two species, we believe it is justified to combine the data sets.

Table 1
Shell growth and seawater chemistry parameters in each experimental setup.

Sample	No. of shells (n)	Total mass		Avg. growth rate $\pm 2\sigma_m$		Seawater					
		Initial (μg)	Final (μg)	(μg/day/ind)	(%/day/ind)	Salinity (psu)	Tem. (°C)	Alkalinity $\pm 2\sigma$ (μeq/l)	C_T $\pm 2\sigma$ (mmol/l)	pH $\pm 2\sigma$ (NBS)	$[CO_3^{2-}]$ $\pm 2\sigma$ (μmol/l)
Globigerinoides ruber experiments 2006											
BK1-32R	2	6.0	41	1.3 ± 0.3	18 ± 9	32.1	24	1964[b]	1.63[b]	8.4[b]	228[b]
BK1-35R	5	12.0	106	2.2 ± 0.3[a]	28 ± 2[a]	35.0	24	2141[b]	1.77[b]	8.3[b]	251[b]
BK1-38R	5	17.8	73	2.2 ± 0.6	27 ± 4	38.0	24	2325[b]	1.92[b]	8.3[b]	276[b]
BK1-41R	3	7.9	55	2.3 ± 0.4	32 ± 4	40.7	24	2490[b]	2.06[b]	8.3[b]	297[b]
BK1-44R	2	5.7	18	1.0 ± 0.4	21 ± 7	44.3	24	2710[b]	2.24[b]	8.3[b]	327[b]
BK2-18R	3	5.5	20	0.61 ± 0.07	17 ± 3	35.0	18	2141[b]	1.77[b]	8.4[b]	249[b]
BK2-21R	4	10.7	40	1.1 ± 0.4	22 ± 6	35.0	21	2141[b]	1.77[b]	8.4[b]	250[b]
BK2-24R	3	10.4	61	2.7 ± 1.4	31 ± 10	35.0	24	2141[b]	1.77[b]	8.3[b]	251[b]
BK2-27R	5	14.8	118	2.9 ± 0.6[a]	32 ± 7[a]	35.0	27	2141[b]	1.77[b]	8.3[b]	252[b]
BK2-30R	6	25.1	168	3.6 ± 0.7	30 ± 3	35.0	30	2141[b]	1.77[b]	8.3[b]	253[b]
BK3-7.9R	2	5.3	29	1.9 ± 0.3	28 ± 2	35.0	27	2040 ± 5	1.85 ± 0.02	7.91 ± 0.06	140 ± 24
BK3-8.1R	3	7.8	88	2.8 ± 0.6	27 ± 3	35.0	27	2133 ± 14	1.85 ± 0.03	8.09 ± 0.08	197 ± 21
BK3-8.3R	3	7.0	76	2.8 ± 1.2	32 ± 2	35.0	27	2259 ± 7	1.86 ± 0.02	8.27 ± 0.07	276 ± 28
BK3-8.4R	2	4.3	59	3.1 ± 1.4	33 ± 16	35.0	27	2423 ± 4	1.87 ± 0.03	8.43 ± 0.08	384 ± 25
Control	9	~43	–	–	–	40.7	22	–	–	–	–
Globigerinella siphonifera experiments 2006											
BK1-32S	2	5.4	60	2.3 ± 0.5	20 ± 4	32.1	24	1964[b]	1.63[b]	8.4[b]	228[b]
BK1-35S	2	5.2	70	3.2 ± 0.2	32 ± 18	35.0	24	2141[b]	1.77[b]	8.3[b]	251[b]
BK1-38S	3	5.7	121	3.6 ± 1.1	35 ± 12	38.0	24	2325[b]	1.92[b]	8.3[b]	276[b]
BK1-41S	2	5.6	63	3.5 ± 1.2	34 ± 7	40.7	24	2490[b]	2.06[b]	8.3[b]	297[b]
BK1-44S _1	3	4.7	156	4.3 ± 0.9	32 ± 3	44.3	24	2710[b]	2.24[b]	8.3[b]	327[b]
BK1-44S _2	3	8.2	141	4.6 ± 1.2	32 ± 7	44.3	24	2710[b]	2.24[b]	8.3[b]	327[b]
BK2-18S	3	5.0	61	1.4 ± 0.3	20 ± 3	35.0	18	2141[b]	1.77[b]	8.4[b]	249[b]
BK2-21S	3	7.2	72	2.3 ± 0.6	25 ± 8	35.0	21	2141[b]	1.77[b]	8.4[b]	250[b]
BK2-24S	2	5.9	82	2.9 ± 0.1	20 ± 3	35.0	24	2141[b]	1.77[b]	8.3[b]	251[b]
BK2-27S	2	2.6	78	3.4 ± 0.5	32 ± 10	35.0	27	2141[b]	1.77[b]	8.3[b]	252[b]
BK2-30S	2	6.9	70	4.5 ± 1.8	34 ± 12	35.0	30	2141[b]	1.77[b]	8.3[b]	253[b]
Globigerinella siphonifera experiments 2007											
BK4-20S	5	18.0	164	2.6 ± 1.1	20 ± 8	40.7	20	2490[b]	2.06[b]	8.3[b]	296[b]
BK4-23S	4	15.2	155	3.7 ± 1.4	28 ± 4	40.7	23	2490[b]	2.06[b]	8.3[b]	297[b]
BK4-26S	3	8.5	73	3.2 ± 0.9	36 ± 5	40.7	26	2490[b]	2.06[b]	8.3[b]	298[b]
BK4-29S	3	10.4	151	4.2 ± 2.2	25 ± 4	40.7	29	2490[b]	2.06[b]	8.2[b]	299[b]
BK4-31S	2	8.9	58	5.9 ± 2.9	43 ± 12	40.7	31	2490[b]	2.06[b]	8.2[b]	299[b]
Control	7	~69	–	–	–	40.7	21.5	–	–	–	–

Total initial mass and total final mass are given for the total number of specimens (n) grouped for each sample. Calcification temperature, salinity and carbonate chemistry parameters are assigned to the control groups using oceanographic data (Shaked and Genin, 2007). B1–B3 experiments were carried out between April and July 2006, whereas B4 experiments were performed between April and May 2007. A detailed explanation of how the average growth rates were calculated is given in Section 2.1.

[a] The average growth rates for these samples were calculated from 6 cultured specimens. One specimen was lost during sample cleaning.

[b] Carbonate system parameters were estimated using the computer program written by Lewis and Wallace (1998) by assuming that total alkalinity (TA) and total inorganic carbon (C_T) are 2490 μeq/l and 2060 μmol/kg, respectively, at a salinity of 40.7 psu in the northern part of the Gulf of Eilat and that TA and C_T behave conservatively with changing salinity.

Table 2
Measured $\delta^{44/40}$Ca and Sr/Ca in cultured *G. ruber* (white) and cultured *G. siphonifera*.

Sample	$\delta^{44/40}$Ca $\pm 2\sigma_m$ [a] (‰)	*n*	Sr/Ca [b] (mmol/mol)
Globigerinoides ruber experiments 2006			
BK1-32R	0.75 ± 0.06	5	1.28
BK1-35R	0.71 ± 0.08	7	1.37
BK1-38R	0.62 ± 0.10	5	1.40
BK1-41R	0.62 ± 0.09	6	1.40
BK1-44R	0.59 ± 0.07	6	-
BK2-18R	0.63 ± 0.10	7	-
BK2-21R	0.69 ± 0.11	5	1.35
BK2-24R	0.72 ± 0.07	8	1.40
BK2-27R	0.74 ± 0.03	6	1.38
BK2-30R	0.63 ± 0.11	7	1.44
BK3-7.9R	0.62 ± 0.12	4	1.42
BK3-8.1R	0.67 ± 0.07	5	1.34
BK3-8.3R	0.70 ± 0.07	5	1.39
BK3-8.4R	0.74 ± 0.12	5	1.37
Control	0.61 ± 0.04	3	1.40
Globigerinella siphonifera experiments 2006			
BK1-32S	0.75 ± 0.08	6	1.22
BK1-35S	0.77 ± 0.14	6	1.24
BK1-38S	0.78 ± 0.03	6	1.25
BK1-41S	0.69 ± 0.04	5	1.31
BK1-44S _1	0.85 ± 0.09	4	1.27
BK1-44S _2	0.81 ± 0.09	5	1.30
BK2-18S	0.82 ± 0.12	4	1.22
BK2-21S	0.86 ± 0.16	5	1.24
BK2-24S	0.70 ± 0.10	5	1.27
BK2-27S	0.86 ± 0.11	5	1.27
BK2-30S	0.80 ± 0.15	5	1.32
Globigerinella siphonifera experiments 2007			
BK4-20S	0.79 ± 0.08	9	1.27
BK4-23S	0.82 ± 0.09	10	1.30
BK4-26S	0.80 ± 0.09	12	1.36
BK4-29S	0.74 ± 0.10	7	1.40
BK4-31S	0.63 ± 0.04	7	1.44
Control	0.73 ± 0.18	3	1.36

[a] $2\sigma_m$ error on $\delta^{44/40}$Ca of each sample was calculated from n number of repeat measurements.
[b] 2σ error on Sr/Ca analysis is estimated as ±0.04 mmol/mol for *G. ruber* and ±0.02 mmol/mol for *G. siphonifera* from the repeats of an internal standard (Section 2.3).

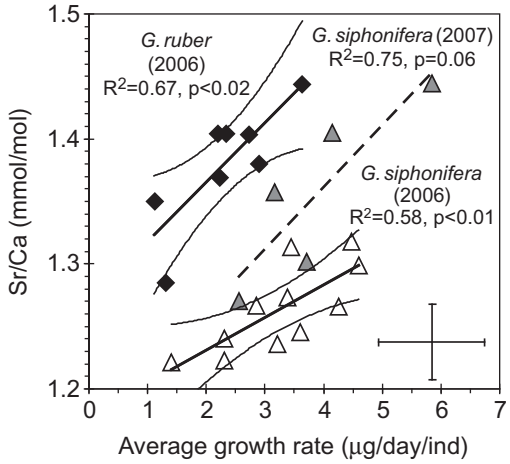

Fig. 3. Growth rate dependence of Sr/Ca in *G. ruber* and *G. siphonifera*. Results of the carbonate chemistry experiments were excluded from the computation of the regression for *G. ruber* (see Section 3.2). The error bars denote average values for 2σ on Sr/Ca (±0.03 mmol/mol) and $2\sigma_m$ on average growth rate (±0.9 µg/day/ind). Please refer to Tables 1 and 2 for detailed information on specific errors. 95% confidence intervals have been plotted for regressions having a better significance level than 5%. The average Sr/Ca ratios of this dataset are 1.38 ± 0.08 mmol/mol (2σ for *G. ruber*, and 1.26 ± 0.07 mmol/mol for *G. siphonifera* (2006 cultures), 1.36 ± 0.14 for *G. siphonifera* (2007 cultures).

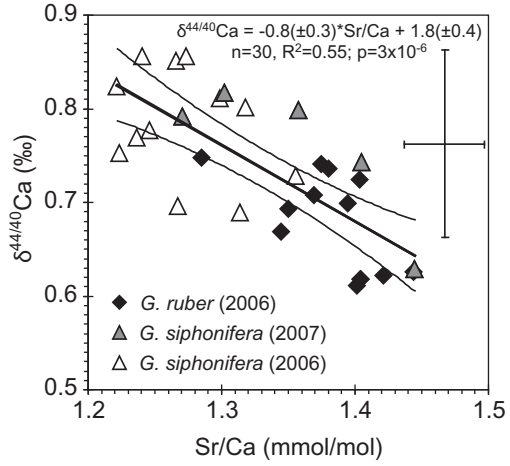

Fig. 4. $\delta^{44/40}$Ca versus Sr/Ca in *G. ruber* (diamonds) and *G. siphonifera* (triangles) for all experiments and control groups (Table 2). The error bar denotes average values for 2σ on Sr/Ca (±0.03 mmol/mol) and $2\sigma_m$ on $\delta^{44/40}$Ca (±0.1‰). Please refer to Table 2 for detailed information on specific errors. The error envelope gives 95% confidence interval for the regression.

4. DISCUSSION

4.1. Controls on $\Delta^{44/40}$Ca and Sr/Ca

In situ analyses of $\delta^{44/40}$Ca in foraminifera revealed >1.5‰ intra-test variability in species of the *globorotaliid* family (Rollion-Bard et al., 2007; Kasemann et al., 2008), possibly associated with differences between the biomineralization pathways of ontogenic versus gametogenetic calcite (see Section 1). The deposition of gametogenetic calcite is negligible in *G. ruber* (Caron et al., 1990) and appears to be small in *G. siphonifera* (Huber et al., 1997). Dissolution experiments on two species of planktic foraminifera (*G. sacculifer* and *N. pachyderma*) revealed relatively constant Ca-isotope ratios (<0.2‰ change in $\delta^{44/40}$Ca for a weight loss of up to 70%), suggesting a homogeneous distribution of Ca-isotope ratios within their tests (Gussone et al., 2009). Additionally, we observed no intra-test variations in Sr/Ca of either species on the electron microprobe. Hence, the relationship observed between Ca isotopes and Sr/Ca is unlikely to be caused by varying thickness of gametogenetic calcite.

Our study does not differentiate between the two main phenotypes (Type I and II) of *G. siphonifera* reported to

be distinct cryptic species (Huber et al., 1997; Section 2.1). Previous genetic sequencing on *G. siphonifera* collected from the Gulf of Eilat at the same time of year as in this study indicates Type II (de Vargas et al., 2002). Higher $\delta^{18}O$ and $\delta^{13}C$ values as well as lower Mg/Ca ratios in Type II compared with Type I have been interpreted as resulting from a deeper depth habitat or a higher photosynthetic rate of symbionts (Huber et al., 1997; Bijma et al., 1998). In addition, biogeographical distribution patterns indicate that Type II is particularly abundant in more mesotrophic environments, suggesting that it may preferentially inhabit the deep chlorophyll maximum layers (de Vargas et al., 2002). So far, there is no study on Ca isotopes (or Sr/Ca) in the two different types of *G. siphonifera*. Overall, we cannot exclude that the trends for *G. siphonifera* may comprise a mixed signal from the two types with potentially different ecologies. However this is not very critical for the interpretation of our data, which show good intra- and inter-species consistency in the observed trends (Figs. 2–4).

4.1.1. Comparison with inorganic precipitation results

Recent experimental observations on inorganically precipitated calcite by Tang et al. (2008a,b,c) revealed that the isotopic fractionation of Ca is strongly correlated with the partitioning of Sr. Tang and coauthors used a pH stat technique with CO_2-diffusion for spontaneous precipitation of calcite in well stirred solutions with Ca and Sr concentrations close to modern seawater (10 and 0.1 mmol/l, respectively). In doing so, the authors showed that the main controls on $^{44}Ca/^{40}Ca$ and Sr/Ca during inorganic calcite formation are intriguingly similar: precipitation rate and temperature. At constant temperature, the degree of Ca isotope fractionation and the partition coefficient of strontium (D_{Sr}) were observed to increase linearly with increasing precipitation rate. Yet, the rate-sensitivity of both $\Delta^{44/40}Ca$ and D_{Sr} were found to decrease with increasing temperature (5, 25 and 40 °C, respectively). Another important observation was that there is a well-defined inverse correlation between $\Delta^{44/40}Ca$ and D_{Sr}, the slope and intercept of which are independent of precipitation rate, temperature, aqueous Sr/Ca and ionic strength of the solution. The authors explained their results by the Surface Entrapment Model, where the isotopic fractionation of Ca is produced under disequilibrium conditions during precipitation by two counteracting mechanisms: (1) the entrapment of a ^{44}Ca depleted surface layer by crystal growth, and (2) the re-equilibration of Ca isotopes in the surface layer of the growing crystal by ion diffusion.

The positive rate dependence of Sr partitioning in inorganically precipitated calcite has been shown by various authors (e.g., Lorens, 1981; Tesoriero and Pankow, 1996; Nehrke et al., 2007; Tang et al., 2008a). The range of D_{Sr} is similar in these studies and varies by about an order of magnitude (approx. from 0.02 to 0.2) with precipitation rates that vary by >2 orders of magnitude (R ~10 to 10,000 μmol/m^2/h). Results of a previous culture experiment on benthic foraminifer *Amphistigina lobifera* and planktic foraminifer *G. sacculifer* at various seawater Sr/Ca ratios found a negative correlation between D_{Sr} and growth at rates lower than ~10%/day, whereas the correlation was positive at growth rates between ~15 and 25%/day (Erez, 2003). The growth rates in our study lie between 17 and 43%/day (Table 1).

The rate dependence of Ca isotope fractionation in inorganic calcite is more controversial. In contrast to Tang et al. (2008b), the experimental results of Lemarchand et al. (2004) showed that the degree of Ca isotope fractionation decreases with increasing precipitation rate at constant temperature. The authors used a pH free drift method for precipitating calcite crystals in unstirred and stirred solutions at two different Ca concentrations (15 and 150 mmol/l, respectively). At constant precipitation rate, larger fractionation was obtained with unstirred solutions compared to stirred solutions. It should be noted that rate was estimated from measured $[CO_3^{2-}]$ using empirical relationships in Lemarchand et al. (2004), whereas it was calculated from the amount of calcite precipitated over the period of growth and the specific surface area in Tang et al. (2008a,b,c). Lemarchand et al. (2004) proposed that the largest isotopic fractionation of Ca occurs at equilibrium. With increasing precipitation rate, the Ca isotope composition of the calcite was suggested to approach that of the solution due to kinetic effects. Stirring was hypothesized to increase precipitation rate via providing more diffusive inflow of CO_3 ions to the crystal lattice. The concept of a large equilibrium Ca isotope fractionation for inorganic calcite was challenged in a later study by Fantle and DePaolo (2007). They showed that marine carbonates and pore fluids that were in chemical equilibrium ($\Omega_{cc} = 1$) over millions of years have identical Ca isotopic compositions. From this observation follows that there is no isotopic fractionation between Ca in calcite and Ca in solution at equilibrium ($\Delta^{44/40}Ca = 0$). This was further confirmed in a study of Ca isotopes in a carbonate aquifer by Jacobson and Holmden (2008).

The contrasting rate-dependence of Ca isotope fractionation reported in Lemarchand et al. (2004) and Tang et al. (2008b) may be related to the stirring strength of the solution. Extensive stirring of the growth solution is hypothesized to reduce the effect of aqueous ion diffusion (Tang et al., 2008b). If so, the results of the experiments with strong stirring would be expected to be more relevant for calcite precipitation under non-stagnant marine conditions.

Our observations are compared to those of Lemarchand et al. (2004) in Fig. 5. The CO_3^{2-} dependence of Ca isotope fractionation in *G. ruber* (determined from carbonate chemistry experiments) has the same slope (0.0005 ± 0.0003 μmol/l/‰) within error as that in inorganically precipitated calcite from stirred solutions (0.0008 ± 0.0004 μmol/l/‰), whereas for a given $[CO_3^{2-}]$ ^{44}Ca discrimination is larger in foraminifera than in inorganic calcite. An important observation is that $\Delta^{44/40}Ca$ in *G. ruber* and *G. siphonifera* cultured at different temperatures and salinities has a much larger spread than can be explained by a possible CO_3^{2-} dependence. In addition, considering that an equilibrium fractionation between calcite and its growth solution has been shown to be close to zero by Fantle and DePaolo (2007) and Jacobson and Holmden (2008), we should investigate other possibilities than the model of Lemarchand et al. (2004) for the interpretation of our results.

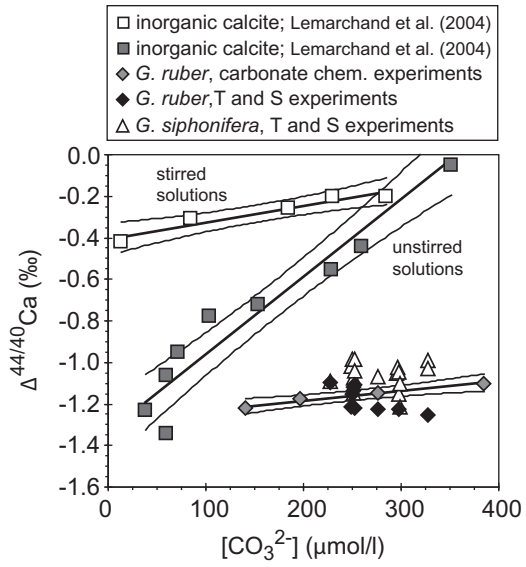

Fig. 5. $\Delta^{44/40}$Ca versus [CO_3^{2-}] in *G. ruber* and *G. siphonifera* compared to that in inorganically precipitated calcite (Lemarchand et al., 2004). 95% confidence intervals have been plotted for each regression.

Our foraminiferal results are compared with the observations of Tang et al. (2008b) in Fig. 6, illustrating that the slope of the correlation between $\Delta^{44/40}$Ca and D_{Sr} in planktic foraminifera is in good agreement with the inorganic calcite data. Foraminiferal regression of $\Delta^{44/40}$Ca versus D_{Sr} has a small but significant positive offset from the inorganic regression, which will be discussed further in Section 4.2. Analogous to the observations of Tang et al. (2008a,b,c), we postulate that Ca isotope fractionation (and Sr partitioning) in the studied foraminifera species is controlled mainly by precipitation kinetics and secondarily by water temperature, explaining the majority of our data set as discussed below.

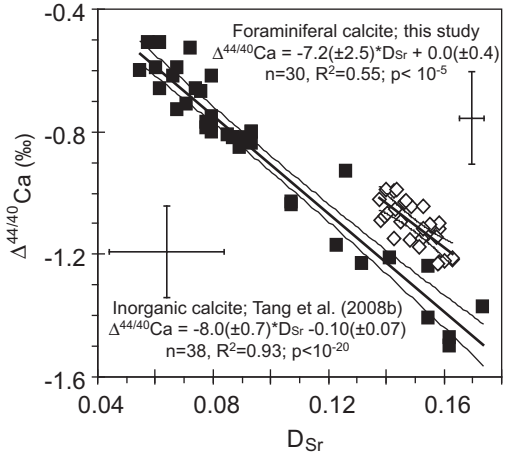

Fig. 6. $\Delta^{44/40}$Ca versus the partition coefficient of Sr (D_{Sr}) in *G. ruber* and *G. siphonifera* (white diamonds) compared to that in inorganically precipitated calcite (black squares; Tang et al., 2008b). The error bar denotes 2σ on D_{Sr} (as estimated from repeats on one sample in Tang et al. (2008a,b,c) and from propagated errors on calcite and the culturing fluid in this study) and $2\sigma_m$ on $\Delta^{44/40}$Ca (as estimated from propagated errors on calcite and the growth solution). The error envelopes give 95% confidence interval for the regressions. "*n*" donates the number of observations.

4.1.2. Precipitation rates in planktic foraminifera

There is no direct way of measuring precipitation rates in foraminifera due to complications related to determining the surface area and estimating the duration of the stepwise calcification process. Thus, generally studies report growth rates (μg/day), providing a measure of the mass increase in foraminifera due to the addition and thickening of chambers over a day. However, planktic foraminifera do not calcify continuously, but only for a few hours each day (Bé et al., 1977). Such an averaging of discontinuous calcification is expected to introduce a large uncertainty in the growth rate calculations. On the other hand, precipitation rate (μmol/m^2/h) is essentially a measure of the instantaneous mass increase over a unit area. Estimates of surface area normalized precipitation rates in planktic foraminifera are essentially based on isotope labelling techniques (Erez, 1983; Anderson and Faber, 1984; Lea et al., 1995) and range from ~40 μmol/m^2/h (Erez, 2003) to as high as 1000–4000 μmol/m^2/h (Carpenter and Lohmann, 1992; Lea et al., 1995). If the sole control on the Ca isotope fractionation in foraminifera is assumed to be inorganic precipitation from an open seawater reservoir, the rate dependence of $\Delta^{44/40}$Ca in inorganic calcite provides us with a unique tool to calculate precipitation rates. At 25 °C water temperature, precipitation rates in *G. siphonifera* and *G. ruber* are calculated to be on the order of 2000 and 3000 μmol/m^2/h, respectively (Fig. 7). We extend our calculation to cultured *O. universa* (Gussone et al., 2003), having a slightly lower precipitation rate of ~1000 μmol/m^2/h (Fig. 7).

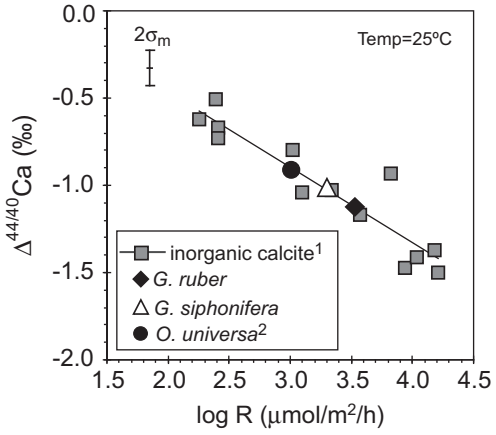

Fig. 7. Observed rate dependence of $\Delta^{44/40}$Ca in inorganic calcite at 25 °C (Tang et al., 2008b). Plotted on the inorganic regression line are the observed $\Delta^{44/40}$Ca values of *G. ruber* and *G. siphonifera* (this study) as well as *O. universa* (Gussone et al., 2003)[2] interpolated to 25 °C, corresponding to precipitation rates of ~3000, 2000 and 1000 μmol/m^2/h, respectively.

At water temperatures exceeding 29 °C, the increased degree of Ca isotope fractionation in *G. ruber* and *G. siphonifera* (by ~0.1–0.2‰; Fig. 2a) deviates from the positive temperature-dependent fractionation trend. Findings of a time-series sediment trap study from the Gulf of California confirmed this observation, showing an even stronger ^{44}Ca depletion ($\Delta^{44/40}Ca < -1.3‰$) in *G. ruber* w. and *G. sacculifer* at temperatures of 30.5–31.1 °C (Griffith et al., 2008). We propose that increased Ca isotope fractionation in planktic foraminifera at these high water temperatures is controlled primarily by increased precipitation rates, as inferred from the negative correlation between precipitation rate and $\Delta^{44/40}$Ca in inorganic calcite (Tang et al., 2008b). This is consistent with the observation that the average growth rate plateaus at $\geqslant$29 °C in the studied species and may be an adaptation strategy of the planktic foraminifera to increased metabolic rates at very high temperatures. Recent O_2 microelectrode work of Lombard et al. (2009a) provides support to this end. The authors showed that both respiration and photosynthesis increase up to 30 °C, the upper limit of their experimental setup, in planktic foraminifera collected from the Gulf of Eilat (*G. ruber* white, *G. siphonifera* and *O. universa*). In contrast, a compilation by Lombard et al. (2009b) revealed a sharp decrease in the growth rates of *G. siphonifera*, *G. ruber* and *O. universa* above 29 °C, based mainly on the culturing work of Bijma et al. (1990) at these high water temperatures. The discrepancy between our observations and those of Bijma et al. (1990) might be due to different phenotypes (*G. ruber* white vs. pink) and habitats (*G. siphonifera* collected from Gulf of Eilat vs. the Caribbean Sea) of the studied foraminifera.

The more pronounced ^{44}Ca depletion in *G. ruber* compared to *G. siphonifera* suggests higher precipitation rates in the former (Fig. 7). Even though the average growth rates are similar for these species (Table 1) differences in precipitation rates might result from their diverse morphologies or distinct durations of calcification. The hypothesized difference in precipitation rates of *G. siphonifera* and *G. ruber* can also explain the lower Sr/Ca ratios in the former species (Fig. 3). A previous study on Sr/Ca in planktic foraminifera from core-tops in the North Atlantic (Elderfield et al., 2000) also found an offset in Sr/Ca between *G. siphonifera* (average: 1.28 ± 0.01 mmol/mol; 1σ) and *G. ruber* (1.43 ± 0.02 mmol/mol). Most other planktic foraminifera species (including *G. sacculifer*, *G. bulloides*, *O. universa*, *N. pachyderma*, *G. menardii*) show fairly constant Sr/Ca ratios for a range of water temperatures between 5 and 20 °C and have mean Sr/Ca values close to that of *G. ruber* (Delaney et al., 1985; Elderfield et al., 2000; Mortyn et al., 2005). This suggests that overall precipitation rates are similar for most species under moderate conditions.

Increasing water temperatures are correlated with increasing Sr/Ca (Fig. 2d). This is in contrast to Sr incorporation into inorganic calcite that decreases with increasing temperature (Tang et al., 2008a and references therein). Thus, calcification temperature appears to have an indirect effect on shell Sr/Ca through its control over precipitation rates (i.e., higher temperatures leading to higher growth rates in planktic foraminifera; Fig. 2g).

Following the above line of reasoning, increasing salinities (at constant temperature) appear to trigger higher precipitation rates in *G. ruber*, resulting in lower $\delta^{44/40}$Ca and higher Sr/Ca (Fig. 2b and e). Although the average growth rate of *G. ruber* is low at 44 psu (Fig. 2h), it is not implausible that the foraminifer is precipitating faster to remove the excess ions at such high salinities while the growth is limited. The lowest $\delta^{44/40}$Ca and highest Sr/Ca in *G. siphonifera* are observed at the salinity of the Gulf of Eilat (41 psu), suggesting that the poor adaptation of this species to lower or higher salinities induces lower precipitation rates.

The positive $[CO_3^{2-}]$ dependence of $\delta^{44/40}$Ca in cultured *G. ruber* (Fig. 2c; having a subtle but significant slope of $0.0005 \pm 0.0003‰/\mu mol/l^{-1}$, $p < 0.02$) cannot be explained by a rate effect according to Tang et al. (2008b). Precipitation rates in calcite are expected to decrease with decreasing $[CO_3^{2-}]$ (Zuddas and Mucci, 1994); this is supported by the low growth rate of *G. ruber* at $[CO_3^{2-}]$ of 140 μmol/l (Fig. 1i). Alternatively, the response of $\delta^{44/40}$Ca to changing seawater $[CO_3^{2-}]$ in *G. ruber* can be explained by the mechanism of pH regulation and cross-membrane transport of Ca ions in the calcification reservoir (Section 4.2.1.1).

Our findings show that coupled $\Delta^{44/40}$Ca and Sr/Ca provide a useful tool for investigating precipitation rates in foraminifera. In addition, our results give evidence that calcification rate is the prime control on Sr partitioning in planktic foraminifera and that temperature and salinity have an indirect effect on shell Sr/Ca through their control over calcification rates (Elderfield et al., 2002; Kısakürek et al., 2008). Thus, our results support the view that Sr/Ca records of planktic foraminifera partly reflect changes in paleoproductivity (Billups et al., 2004). Future work should focus on obtaining coupled $\Delta^{44/40}$Ca and Sr/Ca data for other species of planktic foraminifera, as well as benthic foraminifera, and producing such results for down-core records.

4.2. The vital effect

The small but constant offset between the inorganic and foraminiferal regressions of $\Delta^{44/40}$Ca versus D_{Sr} (as shown by the error envelopes in Fig. 6) has some interesting implications. We exclude an analytical bias in Ca isotope data between this study and Tang et al. (2008b) since all analyses were done in the same laboratory. The error introduced to $\Delta^{44/40}$Ca due to different fluid compositions in this study and Tang et al. (2008b) is on the order of ±0.08‰ ($2\sigma_m$), which is less than the offset between the two regressions (~0.2‰ at constant D_{Sr}) in Fig. 6. On the other hand, we can not completely rule out a consistent analytical bias in Sr/Ca measurements between this study and Tang et al. (2008a) since the analyses were done in different laboratories using different methods (ICP-MS vs. ICP-OES). For a given $\Delta^{44/40}$Ca, D_{Sr} in foraminiferal calcite is ~0.03 higher than that in inorganic calcite. This corresponds to an offset of ~0.25 mmol/mol in Sr/Ca, which is well beyond the typical precision ($2\sigma = \pm 0.05$; Kısakürek et al., 2008). Therefore, we consider the observed offset a vital effect rather than an analytical artefact. Below we will consider two

possible mechanisms for this vital effect: pH modification of vacuolated seawater in planktic foraminifera and/or Rayleigh fractionation from an internal biomineralization reservoir.

4.2.1. pH modification of vacuolated seawater

The concentration of Ca is maintained very low within the cytoplasm (<0.1 μmol/l compared to ~10 mmol/l in seawater) because Ca is an important component of intracellular signalling system (e.g., Hepler and Wayne, 1985). Pulse-chase experiments using fluorescent tracers have shown that foraminifera vacuolate seawater to supply ions (Ca and possibly carbonate) for the bulk of the calcification process (Erez, 2003; Toyofuku et al., 2008) and that the pH of seawater in these vacuoles is elevated to ⩾8.7 against a cytosolic pH of ~7.2 (Erez, 2003; de Nooijer et al., 2008, 2009; Bentov et al., 2009). Since these tracer techniques are limited to a pH range of 6.0 to ~8.5–9.0, the actual pH of the vacuoles might be even higher.

The concentration of Ca in seawater is 10.4 mmol/l while $[CO_3^{2-}]$ is much lower (~0.3 mmol/l); hence, $[CO_3^{2-}]$ is the limiting factor for the precipitation of $CaCO_3$. Elevating the pH in the vacuoles would cause an increase in $[CO_3^{2-}]$, but $[CO_3^{2-}]$ cannot match $[Ca^{2+}]$ at the total inorganic carbon concentration of seawater (~2 mmol/l). However, the high pH level inside the vacuoles is considered to enable metabolic CO_2(aq) to diffuse into the vacuole, forming a carbon pool for the continued calcification process (ter Kuile and Erez, 1987, 1988). Additionally, the increased pH of seawater has been shown to overcome magnesium (Mg) inhibition of calcite precipitation (Zeebe and Sanyal, 2002). Still, the calcite shells of planktic foraminifera have Mg concentrations about a factor of 10 smaller than in inorganic calcite. Thus, these organisms must be actively reducing the Mg concentration at the site of calcification, making their shells less soluble (Bentov and Erez, 2006).

Comparing their results with Lorens (1981) and Tesoriero and Pankow (1996), Tang et al. (2008a) observed that at a constant rate of ~1000 μmol/m^2/h and temperature of 25 °C, D_{Sr} increases by ~0.06 when pH is increased from 6.1 to 8.3. The higher D_{Sr} in foraminifera compared to inorganic calcite (Fig. 6) appears to be consistent with elevated pH of ⩾8.5 in the calcifying vacuoles. Alternatively, the difference between D_{Sr} in foraminiferal and inorganic calcite can be explained via Rayleigh fractionation from a semi-closed seawater reservoir (Section 4.2.2).

4.2.1.1. Cross-membrane transport. The observation that ^{44}Ca discrimination decreases with increasing $[CO_3^{2-}]$ in cultured *G. ruber* (Fig. 2c) is consistent with the mechanism of vacuolar pH regulation. If vacuolization of seawater is assumed to be the main pathway of calcification, then the foraminiferan has to spend more energy at lower pH (or $[CO_3^{2-}]$) of the parent solution in order to elevate the pH of its vacuole. Assuming that pH is at least partly raised by a Ca-ATPase (Erez, 2003), cross-membrane transport of Ca and associated dehydration process are expected to supply more isotopically light Ca into the vacuole at lower seawater pH (Gussone et al., 2006). Thus, a secondary pathway for the transport of Ca ions to the reservoir via active transport through channels and pumps may play an additional role for the observed Ca-isotope ratios of the foraminifer shells. Extrapolating the carbonate chemistry trend of $\delta^{44/40}$Ca in *G. ruber* (using the correlation in Fig. 2c) from ambient seawater pH (~8.2) to a vacuolar pH of ~9 suggests that the fractionation associated with the cross-membrane transport is on the order of −0.2‰. The presence of a pre-fractionated Ca reservoir (with $\delta^{44/40}$Ca of approximately −0.2‰ to −0.4‰ relative to seawater) in foraminifera can resolve the difference in $\Delta^{44/40}$Ca between foraminiferal calcite and other biogenic calcite materials (Gussone et al., 2005) as well as inorganic calcite precipitated over a temperature range of 5–30 °C (Marriott et al., 2004). Alternatively, the difference in $\Delta^{44/40}$Ca of these different calcite materials can be attributed to different rates of precipitation. Although precipitation rate was kept constant, its actual value was not determined by Marriott et al. (2004). Recently, the steep slope of $\delta^{44/40}$Ca-temperature calibration in *G. sacculifer* has been explained via temperature-dependent mixing of the two proposed reservoirs described above; (i) Ca supplied via seawater vacuolization and (ii) Ca supplied across channels and pumps (Gussone et al., 2009). In this model, the trans-membrane contribution of Ca in *G. sacculifer* was calculated to increase from 10% at 29 °C to 50% at 23 °C, suggesting more energy consumption by the organism at lower temperatures for supplying Ca. If such a trans-membrane pathway is valid for the supply of ions into the calcification reservoir, the Sr content of this reservoir might also be modified due to leakage of Sr through the Ca-pump (i.e., ion selectivity; Aidley and Stanfield, 1996). Moreover, if the internal Ca reservoir of foraminifera is fractionated in its isotopic composition relative to seawater, the true offset between the inorganic and foraminiferal regressions should be even larger than that shown in Fig. 6. However, the proposed fractionation of Ca isotopes across membranes, the existence of Ca-ATPase in foraminifera and an associated modification of Sr/Ca in the reservoir remain to be confirmed.

4.2.2. Rayleigh fractionation

An important consideration regarding biomineralization from an internal vacuole system is the effect of Rayleigh distillation. The chemistry of this reservoir is expected to be similar to seawater given that seawater vacuolization is the main supply of ions. If all of the Ca in the vacuole system is used up for calcification, then the average Sr/Ca and ^{44}Ca/^{40}Ca of the calcite is expected to be the same as that of the vacuolated seawater. Alternatively, if very little of the Ca is utilized from the vacuole system, Sr/Ca and ^{44}Ca/^{40}Ca of the calcite is expected to be very close to the open system inorganic values, as observed in this study (Fig. 6).

Elderfield et al. (1996) used a Rayleigh distillation model to explain trace element incorporation into the calcite of benthic foraminifera. Using a constant value for D_{Sr} (0.044), the authors calculated that >90% of the Ca in the reservoir must be incorporated into the calcite shell. However, the inorganic D_{Sr} value adopted by Elderfield and coauthors is on the low end of the published range (~0.02 to 0.2; Section 4.1.1) and does not account for the rate

and temperature dependence of D_{Sr}. Griffith et al. (2008) adopted the Rayleigh distillation model to explain Ca isotope fractionation in planktic foraminifera. The inorganic fractionation factor, $\alpha(^{44}Ca/^{40}Ca)$, was assumed to be dependent only on temperature, disregarding a rate dependence. By adapting a high percentage of Ca utilization (~85%) from the calcification reservoir, Griffith et al. (2008) constrained the $\delta^{44/40}Ca$ value of the foraminiferal reservoir to be −0.85‰ relative to seawater. Our estimate for a potential fractionated Ca reservoir is more moderate; i.e., in the order of −0.2‰ relative to seawater as explained in detail in Section 4.2.1.1.

We apply the Rayleigh distillation model to coupled $\delta^{44/40}Ca$ and Sr/Ca (Eqs. (3) and (4)). The inorganic partition coefficient of strontium, D'_{Sr}, and the inorganic fractionation factor of Ca isotopes, $\alpha(^{44}Ca/^{40}Ca)$, are assumed to be correlated as shown in Eq. (5) (Tang et al., 2008b), accounting for the rate and temperature dependence on both proxies. This approach allows us to solve for the fraction of Ca remaining (f) in the reservoir.

$$[^{44}Ca/^{40}Ca]_{foram}/[^{44}Ca/^{40}Ca]_{reservoir} = (1 - f^{\alpha(^{44}Ca/^{40}Ca)})/(1 - f) \quad (3)$$

$$[Sr/Ca]_{foram}/[Sr/Ca]_{reservoir} = (1 - f^{D'_{Sr}})/(1 - f) \quad (4)$$

$$[\alpha(^{44}Ca/^{40}Ca) - 1] * 1000 = -1.90 * \log D'_{Sr} - 2.83 \quad (5)$$

If the Ca isotope composition of the reservoir is assumed to be the same as that of seawater ($\delta^{44/40}Ca_{reservoir} = \delta^{44/40}Ca_{seawater}$), the calculated range of f values is 0.81–0.92 for *G. ruber* and 0.76–0.92 for *G. siphonifera*, indicating less than 25% of the Ca supplied by the vacuolization system is utilized for calcite precipitation. If the Ca isotope composition of the reservoir is assumed to be somewhat fractionated relative to seawater ($\delta^{44/40}Ca_{reservoir} = \delta^{44/40}Ca_{seawater} - 0.2‰$), the calculated range of f values is 0.64–0.74 for *G. ruber* and 0.58–0.72 for *G. siphonifera*. Our calculations suggest that even with a pre-fractionated reservoir, less than half of the Ca supplied by the vacuolization system is utilized for calcite precipitation.

On the whole, it appears that the vacuole system behaves as a semi-open system in planktic foraminifera. This is in line with the observations that the site of biomineralization is not completely separated from the ambient seawater, but rather confined by reticulated pseudopodia, i.e., extrusions of the cell (Erez, 2003). It follows that the vacuoles, modified in their chemistry by the organism, are eventually exocytosed into the site of biomineralization, which has exchange with seawater (Erez, 2003).

4.3. Comparison with other low-Mg calcifiers

Fig. 8 illustrates the correlation between $\Delta^{44/40}Ca$ and D_{Sr} in inorganic calcite as well as in the skeletons of various marine organisms secreting low-Mg calcite. Even though the skeletal $\Delta^{44/40}Ca$ values of marine organisms are within the inorganic range, the biogenic spread in D_{Sr} appears wider than the inorganic variability.

Data on brachiopods (Steuber and Buhl, 2006; Farkaš et al., 2007), blue mussels (Heinemann et al., 2008) and

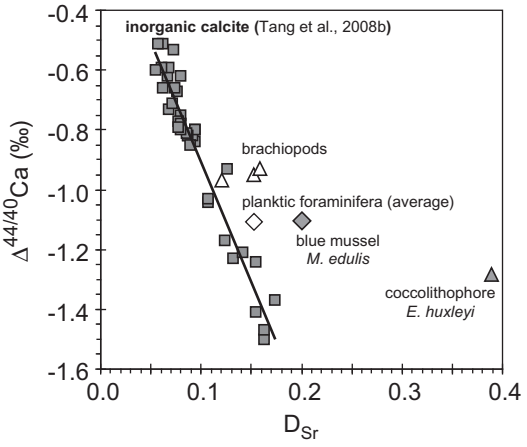

Fig. 8. Calcium isotope fractionation versus partition coefficient of Sr in low-Mg calcite (with Mg/Ca ratios of <10 mmol/mol): inorganic calcite (gray squares; Tang et al., 2008b), low-Mg calcite of brachiopods (white triangles; Steuber and Buhl, 2006; Farkaš et al., 2007), blue mussel *Mytilus edulis* (gray diamond, where $\Delta^{44/40}Ca$ and D_{Sr} are plotted relative to the extrapallial fluid; Heinemann et al., 2008), average planktic foraminifer (white diamond; this study) and coccolithophore *Emiliania huxleyi* (gray triangle; Langer et al., 2006, 2007).

planktic foraminifera (this study) plot close to the inorganic regression line (Tang et al., 2008b), with a small positive offset in D_{Sr}. It must be noted that $\Delta^{44/40}Ca$ and D_{Sr} of brachiopods and planktic foraminifera are reported relative to seawater, whereas those of the blue mussel, *Mytilus edulis*, are reported relative to the extrapallial fluid. In addition, the data on brachiopods coincide with the average of foraminifera if a pre-fractionated Ca reservoir with $\delta^{44/40}Ca$ of approximately −0.2‰ to −0.4‰ relative to seawater is assumed for the latter. In line with our preceding discussion, these data suggest a semi-open calcification system with a primarily kinetic control with regards to Ca and Sr incorporation in these organisms. Thus, in this first group of calcifiers, paired $\Delta^{44/40}Ca$ and D_{Sr} might be utilized to determine biogenic precipitation rates, a parameter that cannot be measured directly.

In contrast, data on coccolithophores (Langer et al., 2006, 2007) show a relatively large offset from the inorganic regression line. Intriguingly, coccolith $\Delta^{44/40}Ca$ is within the range of inorganic values and other biogenic data, whereas D_{Sr} is much higher than the inorganic spread. Thus, the controls on Sr incorporation appear to be uncoupled from those on Ca isotope fractionation in coccolithophores. The calcification process in coccolithophores takes place within a confined vesicle similar in volume to a single coccolith (e.g., Young and Henriksen, 2003) and the Ca uptake into this vesicle is thought to be accomplished via trans-membrane transport using Ca channels and ATPases (Brownlee and Taylor, 2004). Enrichment of Sr/Ca in the coccolith calcite compared to inorganic calcite has been explained using a simple conceptual model based on the channel-mediated transport of Ca and Sr to the coccolith vesicle (Langer et al., 2006, 2009). In addition, the positive correlation between D_{Sr} and calcification rates in coccolithophores

(Stoll and Schrag, 2000) has been explained by a rate-dependent discrimination between the biological transport of Sr and Ca ions (Rickaby et al., 2002).

Overall, it appears that Ca isotope composition and Sr/Ca ratios in the calcite of marine organisms are useful tools for examining the pathways of Ca transport (i.e., vacuolization from seawater and/or active transport through channels and pumps) to the site of calcification. Future work should aim at investigating other trace elements and their isotopic compositions (e.g., Mg and its isotopes) in both low-Mg and high-Mg secreting marine calcifiers as a means to study distinct pathways of biomineralization.

5. SUMMARY AND CONCLUSIONS

We analyzed Ca isotopes and Sr/Ca ratios in planktic foraminifera *Globigerinoides ruber* (white) and *Globigerinella siphonifera* grown under controlled laboratory conditions at different salinity, temperature and $[CO_3^{2-}]$ values. Overall, the total variations in $\delta^{44/40}Ca$ ($\sim$0.3‰) and Sr/Ca (0.22 mmol/mol) are small revealing a tight control of the organism on its shell chemistry. On the other hand, the variations in the data show distinct trends and are controlled by more than one environmental parameter. There is a significant inverse correlation between Sr/Ca and $\delta^{44/40}Ca$ in *G. ruber* and *G. siphonifera*, in line with recent observations from inorganically precipitated calcite (Tang et al., 2008a,b,c). Indeed the regressions of $\Delta^{44/40}Ca$ versus D_{Sr} are very similar for foraminiferal and inorganic calcite, with a small but significant positive offset in the former. These results indicate that Ca isotope fractionation (and Sr partitioning) in planktic foraminifera has similar controls as in inorganic calcite; namely kinetics and temperature (Tang et al., 2008a,b). This postulation is further supported by our observation that Sr/Ca is strongly correlated with average growth rate in the studied foraminifera species. We conclude that:

- Higher Sr/Ca and lower $\delta^{44/40}Ca$ in *G. ruber* compared to *G. siphonifera* are consistent with higher precipitation rates in the former. At a water temperature of 25 °C, precipitation rates in *G. ruber* and *G. siphonifera* are estimated as $\sim$3000 and 2000 μmol/m^2/h, respectively. Below 27 °C, Ca isotope fractionation in *G. ruber* is temperature dependent, showing a sensitivity of $\sim$0.02‰/°C. Water temperatures exceeding 29 °C appear to induce high precipitation rates in *G. ruber* and *G. siphonifera*, causing a high degree of fractionation in Ca isotopes.
- *G. siphonifera* appears to be well adapted to the salinity of Gulf of Eilat (41 psu) and has higher $\delta^{44/40}Ca$ (and lower Sr/Ca) at lower or higher salinities presumably due to decreased precipitation rates. Increasing salinities seem to trigger higher precipitation rates in *G. ruber*, resulting in decreasing $\delta^{44/40}Ca$ (and increasing Sr/Ca).
- The offset between foraminiferal and inorganic regressions of $\Delta^{44/40}Ca$ versus D_{Sr} is consistent with one or both of two scenarios: (i) elevated pH of $\sim$9 in the calcifying vacuoles of foraminifera leading to an increase of D_{Sr} in the shell; and/or (ii) Rayleigh-type fractionation from a semi-open biomineralization system, leading to an increase in both $\Delta^{44/40}Ca$ and D_{Sr} simultaneously, where less than half of the Ca supplied by the vacuolization system is used for calcite precipitation.
- The positive $[CO_3^{2-}]$ dependence of $\delta^{44/40}Ca$ in cultured *G. ruber* cannot be explained by a rate effect, but it is compatible with the mechanism of vacoular pH regulation during biomineralization.

ACKNOWLEDGMENTS

This work was funded by the German Science Foundation (DFG Ei272/21-1), the European Science Foundation (ESF) Collaborative Research Project CASIOPEIA (04 ECLIM FP08) and the Israel Science Foundation (Grant # 870/05). E.C.H. was funded by a MARUM fellowship. The field work was carried out at the IUI-Eilat, with the assistance of Moty Ohavia, Oded Ben Shaprut and Tanya Rivlin in collection of planktic foraminifera and the culturing experiments. We would like to thank Ulrike Westernströer and Dieter Garbe-Schönberg for mass spectrometric analysis and Ana Kolevica for her assistance in the laboratory. We are grateful to three anonymous reviewers for their helpful comments as well as A. Cohen for the editorial handling.

REFERENCES

Aidley D. J. and Stanfield P. R. (1996) *Ion Channels – Molecules in Action*. Cambridge University Press, Cambridge. pp. 307.

Amini M., Eisenhauer A., Böhm F., Fietzke J., Bach W., Garbe-Schönberg D., Rosner M., Bock B., Lackschewitz K. S. and Hauff F. (2008) Calcium isotope ($\delta^{44/40}Ca$) fractionation along hydrothermal pathways, Logatchev field (Mid-Atlantic Ridge, 14 45′N). *Geochim. Cosmochim. Acta* **72**, 4107–4122.

Anderson O. R. and Faber W. W. (1984) An estimation of calcium carbonate deposition rate in a planktonic foraminifer *Globigerinoides sacculifer* using ^{45}Ca as a tracer – a recommended procedure for improved accuracy. *J. Foramin. Res.* **14**, 303–308.

Bé A. W. H., Hemleben C., Anderson O. R., Spindler M., Hacunda J. and Tuntivate-Choy S. (1977) Laboratory and field observations of living planktonic foraminifera. *Micropaleontology* **23**, 155–179.

Bentov S. and Erez J. (2006) Impact of biomineralization processes on the Mg content of foraminiferal shells: a biological perspective. *Geochem. Geophys. Geosys.* **7**. doi:10.1029/2005GC001015.

Bentov S., Brownlee C. and Erez J. (2009) The role of seawater endocytosis in the biomineralization process in calcareous foraminifera. *Proc. Natl. Acad. Sci. USA* **106**, 21500–21504.

Bijma J., Faber W. W. and Hemleben C. (1990) Temperature and salinity limits for growth and survival of some planktonic foraminifers in laboratory cultures. *J. Foramin. Res.* **20**, 95–116.

Bijma J., Hemleben C., Huber B. T., Erlenkeuser H. and Kroon D. (1998) Experimental determination of the ontogenetic stable isotope variability in two morphotypes of *Globigerinella siphonifera* (d'Orbigny). *Mar. Micropaleontol.* **35**, 141–160.

Billups K., Rickaby R. E. M. and Schrag D. P. (2004) Cenozoic pelagic Sr/Ca records: exploring a link to paleoproductivity. *Paleoceanography* **19**. doi:10.1029/2004PA001011.

Böhm F., Gussone N., Eisenhauer A., Dullo C., Reynaud S. and Paytan A. (2006) Calcium isotope fractionation in modern scleractinian corals. *Geochim. Cosmochim. Acta* **70**, 4452–4462.

Brownlee C. and Taylor A. (2004) Calcification in coccolithophores: a cellular perspective. In *Coccolithophores – From Molecular Processes to Global Impact* (eds. H. R. Thiersteinand and J. R. Young). Springer, New York, pp. 31–40.

Caron D. A., Anderson O. R., Lindsey J. L., Faber W. W. and Lim E. L. (1990) Effects of gametogenesis on test structure and dissolution of some spinose planktonic-foraminifera and implications for test preservation. *Mar. Micropaleontol.* **16**, 93–116.

Carpenter S. J. and Lohmann K. C. (1992) Sr/Mg ratios of modern marine calcite – empirical indicators of ocean chemistry and precipitation rate. *Geochim. Cosmochim. Acta* **56**, 1837–1849.

Chang V. T. C., Williams R. J. P., Makishima A., Belshawl N. S. and O'Nions R. K. (2004) Mg and Ca isotope fractionation during $CaCO_3$ biomineralisation. *Biochem. Biophys. Res. Commun.* **323**, 79–85.

Darling K. F., Wade C. M., Kroon D. and Brown A. J. L. (1997) Planktic foraminiferal molecular evolution and their polyphyletic origins from benthic taxa. *Mar. Micropaleontol.* **30**, 251–266.

Darling K. F. and Wade C. A. (2008) The genetic diversity of planktic foraminifera and the global distribution of ribosomal RNA genotypes. *Mar. Micropaleontol.* **67**, 216–238.

De La Rocha C. L. and DePaolo D. J. (2000) Isotopic evidence for variations in the marine calcium cycle over the Cenozoic. *Science* **289**, 1176–1178.

de Nooijer L. J., Toyofuku T., Oguri K., Nomaki H. and Kitazato H. (2008) Intracellular pH distribution in foraminifera determined by the fluorescent probe HPTS. *Limnol. Oceanogr. Meth.* **6**, 610–618.

de Nooijer L. J., Toyofuku T. and Kitazato H. (2009) Foraminifera promote calcification by elevating their intracellular pH. *Proc. Natl. Acad. Sci. USA* **106**, 15374–15378.

de Vargas C., Bonzon M., Rees N. W., Pawlowski J. and Zaninetti L. (2002) A molecular approach to biodiversity and biogeography in the planktonic foraminifer *Globigerinella siphonifera* (d'Orbigny). *Mar. Micropaleontol.* **45**, 101–116.

Delaney M. L., Bé A. W. H. and Boyle E. A. (1985) Li, Sr, Mg, and Na in foraminiferal calcite shells from laboratory culture, sediment traps and sediment cores. *Geochim. Cosmochim. Acta* **49**, 1327–1341.

Dickson A. G. and Millero F. J. (1987) A comparison of the equilibrium constants for the dissociation of carbonic acid in seawater media. *Deep-Sea Res.* **34**, 1733–1743.

Dickson A. G. (1990) Standard Potential of the Reaction $(AgCl(s) + 1/2H_2\ (g) = Ag(s) + HCl(aq))$ and the standard acidity constant of bisulfate ion in synthetic sea water from 273.15 K to 318.15 K. *J. Chem. Thermodyn.* **22**, 113–127.

Eisenhauer A., Nägler T. F., Stille P., Kramers J., Gussone N., Bock B., Fietzke J., Hippler D. and Schmitt A. D. (2004) Proposal for international agreement on Ca notation resulting from discussions at workshops on stable isotope measurements held in Davos (Goldschmidt 2002) and Nice (EGS-AGU-EUG 2003). *Geostand. Geoanal. Res.* **28**, 149–151.

Elderfield H., Bertram C. J. and Erez J. (1996) A biomineralization model for the incorporation of trace elements into foraminiferal calcium carbonate. *Earth Planet. Sci. Lett.* **142**, 409–423.

Elderfield H., Cooper M. and Ganssen G. (2000) Sr/Ca in multiple species of planktonic foraminifera: implications for reconstructions of seawater Sr/Ca. *Geochem. Geophys. Geosys.* **1**, **1999GC000031**.

Elderfield H., Vautravers M. and Cooper M. (2002) The relationship between shell size and Mg/Ca, Sr/Ca, $\delta^{18}O$, and $\delta^{13}C$ of species of planktonic foraminifera. *Geochem. Geophys. Geosys.* **3**. doi:10.1029/2001GC000194.

Erez J. (1983) Calcification rates, photosynthesis and light in planktonic foraminifera. In *Biomoneralization and Biological Metal Accumulation* (eds. P. Westbroekand and E. W. de Jong). D. Reidel Publishing Company, Dordrecht, pp. 307–312.

Erez J. (2003) The source of ions for biomineralization in foraminifera and their implications for paleoceanographic proxies. *Rev. Mineral. Geochem.* **54**, 115–149.

Faber W. W., Anderson O. R., Lindsey J. L. and Caron D. A. (1988) Algal-foraminiferal symbiosis in the planktonic foraminifer *Globigerinella aequilateralis*: 1. Occurrence and stability of 2 mutually exclusive chrysophyte endosymbionts and their ultrastructure. *J. Foramin. Res.* **18**, 334–343.

Faber W. W., Anderson O. R. and Caron D. A. (1989) Algal-foraminiferal symbiosis in the planktonic foraminifer *Globigerinella aequilateralis*: 2. Effects of 2 symbiont species on foraminiferal growth and longevity. *J. Foramin. Res.* **19**, 185–193.

Fantle M. S. and DePaolo D. J. (2007) Ca isotopes in carbonate sediment and pore fluid from ODP Site 807A: the $Ca^{2+(aq)}$ calcite equilibrium fractionation factor and calcite recrystallization rates in Pleistocene sediments. *Geochim. Cosmochim. Acta* **71**, 2524–2546.

Farkaš J., Buhl D., Blenkinsop J. and Veizer J. (2007) Evolution of the oceanic calcium cycle during the late Mesozoic: evidence from $\delta^{44/40}Ca$ of marine skeletal carbonates. *Earth Planet. Sci. Lett.* **253**, 96–111.

Greaves M., Barker S., Daunt C. and Elderfield H. (2005) Accuracy, standardization, and interlaboratory calibration standards for foraminiferal Mg/Ca thermometry. *Geochem. Geophys. Geosys.* **6**. doi:10.1029/2004GC000790.

Griffith E. M., Paytan A., Kozdon R., Eisenhauer A. and Ravelo A. C. (2008) Influences on the fractionation of calcium isotopes in planktonic foraminifera. *Earth Planet. Sci. Lett.* **268**, 124–136.

Gussone N., Eisenhauer A., Heuser A., Dietzel M., Bock B., Böhm F., Spero H. J., Lea D. W., Bijma J. and Nägler T. F. (2003) Model for kinetic effects on calcium isotope fractionation ($\delta^{44}Ca$) in inorganic aragonite and cultured planktonic foraminifera. *Geochim. Cosmochim. Acta* **67**, 1375–1382.

Gussone N., Eisenhauer A., Tiedemann R., Haug G. H., Heuser A., Bock B., Nägler T. F. and Muller A. (2004) Reconstruction of Caribbean sea surface temperature and salinity fluctuations in response to the pliocene closure of the Central American Gateway and radiative forcing, using $\delta^{44/40}Ca$, $\delta^{18}O$ and Mg/Ca ratios. *Earth Planet. Sci. Lett.* **227**, 201–214.

Gussone N., Böhm F., Eisenhauer A., Dietzel M., Heuser A., Teichert B. M. A., Reitner J., Worheide G. and Dullo W. C. (2005) Calcium isotope fractionation in calcite and aragonite. *Geochim. Cosmochim. Acta* **69**, 4485–4494.

Gussone N., Langer G., Thoms S., Nehrke G., Eisenhauer A., Riebesell U. and Weber G. (2006) Cellular calcium pathways and isotope fractionation in *Emiliania huxleyi*. *Geology* **34**, 625–628.

Gussone N., Langer G., Geisen M., Steel B. A. and Riebesell U. (2007) Calcium isotope fractionation in coccoliths of cultured *Calcidiscus leptoporus*, *Helicosphaera carteri*, *Syracosphaera pulchra* and *Umbilicosphaera foliosa*. *Earth Planet. Sci. Lett.* **260**, 505–515.

Gussone N., Hönish B., Heuser A., Eisenhauer A., Spindler M. and Hemleben C. (2009) A critical evaluation of calcium isotope ratios in tests of planktonic foraminifers. *Geochim. Cosmochim. Acta* **73**, 7241–7255.

Heinemann A., Fietzke J., Eisenhauer A. and Zumholz K. (2008) Modification of Ca isotope and trace metal composition of the major matrices involved in shell formation of *Mytilus edulis*. *Geochem. Geophys. Geosys.* **9**. doi:10.1029/2007GC001777.

Hemleben C., Spindler M., Breitinger I. and Ott R. (1987) Morphological and physiological responses of *Globigerinoides*

sacculifer (Brady) under varying laboratory conditions. *Mar. Micropaleontol.* **12**, 305–324.

Hemleben C., Spindler M. and Anderson O. R. (1989) *Modern Planktonic Foraminifera*. Springer-Verlag, New York. pp. 363.

Hepler P. K. and Wayne R. O. (1985) Calcium and plant development. *Ann. Rev. Plant Physiol.* **36**, 397–439.

Heuser A., Eisenhauer A., Gussone N., Bock B., Hansen B. T. and Nägler T. F. (2002) Measurement of calcium isotopes (δ^{44}Ca) using a multicollector TIMS technique. *Int. J. Mass Spectrom.* **220**, 385–397.

Heuser A., Eisenhauer A., Böhm F., Wallmann K., Gussone N., Pearson P. N., Nägler T. F. and Dullo W.-C. (2005) Calcium isotope ($\delta^{44/40}$Ca) variations of Neogene planktonic foraminifera. *Paleoceanography* **20**. doi:10.1029/2004PA001048.

Hippler D., Schmitt A. D., Gussone N., Heuser A., Stille P., Eisenhauer A. and Nägler T. F. (2003) Calcium isotopic composition of various reference materials and seawater. *Geostand. Newslett.* **27**, 13–19.

Hippler D., Eisenhauer A. and Nägler T. F. (2006) Tropical Atlantic SST history inferred from Ca isotope thermometry over the last 140 ka. *Geochim. Cosmochim. Acta* **70**, 90–100.

Hippler D., Kozdon R., Darling K. F., Eisenhauer A. and Nägler T. F. (2009) Calcium isotopic composition of high-latitude proxy carrier *Neogloboquadrina pachyderma* (sin.). *Biogeosciences* **6**, 1–14.

Huber B. T., Bijma J. and Darling K. (1997) Cryptic speciation in the living planktonic foraminifer *Globigerinella siphonifera* (d'Orbigny). *Paleobiology* **23**, 33–62.

Jacobson A. D. and Holmden C. (2008) δ^{44}Ca evolution in a carbonate aquifer and its bearing on the equilibrium isotope fractionation factor for calcite. *Earth Planet. Sci. Lett.* **270**, 349–353.

Kasemann S. A., Schmidt D. N., Pearson P. N. and Hawkesworth C. J. (2008) Biological and ecological insights into Ca isotopes in planktic foraminifers as a palaeotemperature proxy. *Earth Planet. Sci. Lett.* **271**, 292–302.

Kısakürek B., Eisenhauer A., Böhm F., Garbe-Schönberg D. and Erez J. (2008) Controls on shell Mg/Ca and Sr/Ca in cultured planktonic foraminiferan, *Globigerinoides ruber* (white). *Earth Planet. Sci. Lett.* **273**, 260–269.

Kozdon R., Eisenhauer A., Weinelt M., Meland M. Y. and Nürnberg D. (2009) Reassessing Mg/Ca temperature calibrations of *Neogloboquarina pacyderma* (sinistral) using paired $\delta^{44/40}$Ca and Mg/Ca measurements. *Geochem. Geophys. Geosys.* **10**. doi:10.1029/2008GC002169.

Langer G., Gussone N., Nehrke G., Riebesell U., Eisenhauer A., Kuhnert H., Rost B., Trimborn S. and Thoms S. (2006) Coccolith strontium to calcium ratios in *Emiliania huxleyi*: the dependence on seawater strontium and calcium concentrations. *Limnol. Oceanogr.* **51**, 310–320.

Langer G., Gussone N., Nehrke G., Riebesell U., Eisenhauer A. and Thoms S. (2007) Calcium isotope fractionation during coccolith formation in *Emiliania huxleyi*: independence of growth and calcification rate. *Geochem. Geophys. Geosys.* **8**. doi:10.1029/2006GC001422.

Langer G., Nehrke G., Thoms S. and Stoll H. M. (2009) Barium partitioning in coccoliths of *Emiliania huxleyi*. *Geochim. Cosmochim. Acta* **73**, 2899–2906.

Lea D. W., Martin P. A., Chan D. A. and Spero H. J. (1995) Calcium uptake and calcification rate in the planktonic foraminifer *Orbulina universa*. *J. Foramin. Res.* **25**, 14–23.

Lemarchand D., Wasserburg G. T. and Papanastassiou D. A. (2004) Rate-controlled calcium isotope fractionation in synthetic calcite. *Geochim. Cosmochim. Acta* **68**, 4665–4678.

Lewis E. and Wallace D. (1998) *Program Developed for CO_2 System Calculations*. Carbon Dioxide Information Analysis Center, Oak Ridge National Laboratory, U.S. Department of Energy.

Lombard F., Erez J., Michel E. and Labeyrie L. (2009a) Temperature effect on respiration and photosynthesis of the symbiont-bearing planktonic foraminifera *Globigerinoides ruber*, *Orbulina universa*, and *Globigerinella siphonifera*. *Limnol. Oceanogr.* **54**, 210–218.

Lombard F., Labeyrie L., Michel E., Spero H. J. and Lea D. W. (2009b) Modelling the temperature dependent growth rates of planktic foraminifera. *Mar. Micropaleontol.* **70**, 1–7.

Lorens R. B. (1981) Sr, Cd, Mn and Co distribution coefficients in calcite as a function of calcite precipitation rate. *Geochim. Cosmochim. Acta* **45**, 553–561.

Marriott C. S., Henderson G. M., Belshaw N. S. and Tudhope A. W. (2004) Temperature dependence of δ^7Li, δ^{44}Ca and Li/Ca during growth of calcium carbonate. *Earth Planet. Sci. Lett.* **222**, 615–624.

Mehrbach C., Culberso Ch., Hawley J. E. and Pytkowic Rm. (1973) Measurement of apparent dissociation constants of carbonic acid in seawater at atmospheric pressure. *Limnol. Oceanogr.* **18**, 897–907.

Mortyn P. G., Elderfield H., Anand P. and Greaves M. (2005) An evaluation of controls on planktonic foraminiferal Sr/Ca: comparison of water column and core-top data from a North Atlantic transect. *Geochem. Geophys. Geosys.* **6**.

Nägler T. F., Eisenhauer A., Müller A., Hemleben C. and Kramers J. (2000) The δ^{44}Ca-temperature calibration on fossil and cultured *Globigerinoides sacculifer*: new tool for reconstruction of past sea surface temperatures. *Geochem. Geophys. Geosys.* **1**, 2000GC000091.

Nehrke G., Reichart G. J., Vanm Cappellen V., Meile C. and Bijma J. (2007) Dependence of calcite growth rate and Sr partitioning on solution stoichiometry: non-Kosse crystal growth. *Geochim. Cosmochim. Acta* **71**, 2240–2249.

Rickaby R. E. M., Schrag D. P., Zondervan I. and Riebesell U. (2002) Growth rate dependence of Sr incorporation during calcification of *Emiliania huxleyi*. *Global Biogeochem. Cycles* **16**. doi:10.1029/2001GB001408.

Rollion-Bard C., Vigier N. and Spezzaferri S. (2007) In situ measurements of calcium isotopes by ion microprobe in carbonates and application to foraminifera. *Chem. Geol.* **244**, 679–690.

Shaked Y. and Genin A. (2007) *Israel National Monitoring Program at the Gulf of Eilat*. Scientific Report 2006. 131pp.

Silverman J., Lazar B. and Erez J. (2007) Community metabolism of a coral reef exposed to naturally varying dissolved inorganic nutrient loads. *Biogeochemistry* **84**, 67–82.

Sime N. G., De La Rocha C. L. and Galy A. (2005) Negligible temperature dependence of calcium isotope fractionation in 12 species of planktonic foraminifera. *Earth Planet. Sci. Lett.* **232**, 51–66.

Sime N. G., De La Rocha C. L., Tipper E. T., Tripati A., Galy A. and Bickle M. J. (2007) Interpreting the Ca isotope record of marine biogenic carbonates. *Geochim. Cosmochim. Acta* **71**, 3979–3989.

Steuber T. and Buhl D. (2006) Calcium-isotope fractionation in selected modern and ancient marine carbonates. *Geochim. Cosmochim. Acta* **70**, 5507–5521.

Stoll H. M. and Schrag D. P. (2000) Coccolith Sr/Ca as a new indicator of coccolithophorid calcification and growth rate. *Geochem. Geophys. Geosys.* **1**, 1–24.

Tang J. W., Köhler S. J. and Dietzel M. (2008a) Sr^{2+}/Ca^{2+} and $^{44}Ca/^{40}Ca$ fractionation during inorganic calcite formation: I. Sr incorporation. *Geochim. Cosmochim. Acta* **72**, 3718–3732.

Tang J. W., Dietzel M., Böhm F., Köhler S. J. and Eisenhauer A. (2008b) Sr^{2+}/Ca^{2+} and $^{44}Ca/^{40}Ca$ fractionation during inor-

ganic calcite formation: II. Ca isotopes. *Geochim. Cosmochim. Acta* **72**, 3733–3745.

Tang J. W., Niedermayr A., Köhler S. J., Dietzel M., Böhm F., Kisakurek B. and Eisenhauer A. (2008c) No impact of ionic strength/salinity on divalent cation fractionation during inorganic calcite precipitation. *Eos Trans. AGU* **89**(53), Fall Meet. Suppl., Abstract B11C-0386.

ter Kuile B. and Erez J. (1987) Uptake of inorganic carbon and internal carbon cycling in symbiont-bearing benthonic foraminifera. *Mar. Biol.* **94**, 499–509.

ter Kuile B. and Erez J. (1988) The size and function of the internal inorganic carbon pool of the foraminifer *Amphistegina lobifera*. *Mar. Biol.* **99**, 481–487.

Tesoriero A. J. and Pankow J. F. (1996) Solid solution partitioning of Sr^{2+}, Ba^{2+}, and Cd^{2+} to calcite. *Geochim. Cosmochim. Acta* **60**, 1053–1063.

Toyofuku T., de Nooijer L. J., Yamamoto H. and Kitazato H. (2008) Real-time visualization of calcium ion activity in shallow benthic foraminiferal cells using the fluorescent indicator Fluo-3 AM. *Geochem. Geophys. Geosys.* **9**. doi:10.1029/2007GC001772.

Young J. R. and Henriksen K. (2003) Biomineralization within vesicles: the calcite of coccoliths. *Rev. Mineral. Geochem.* **54**, 189–215.

Zeebe R. E. and Sanyal A. (2002) Comparison of two potential strategies of planktonic foraminifera for house building: Mg^{2+} or H^+ removal? *Geochim. Cosmochim. Acta* **66**, 1159–1169.

Zhu P. and Macdougall J. D. (1998) Calcium isotopes in the marine environment and the oceanic calcium cycle. *Geochim. Cosmochim. Acta* **62**, 1691–1698.

Zuddas P. and Mucci A. (1994) Kinetics of calcite precipitation from seawater. 1. A classical chemical-kinetics description for strong electrolyte-solutions. *Geochim. Cosmochim. Acta* **58**, 4353–4436.

Associate editor: Anne Cohen